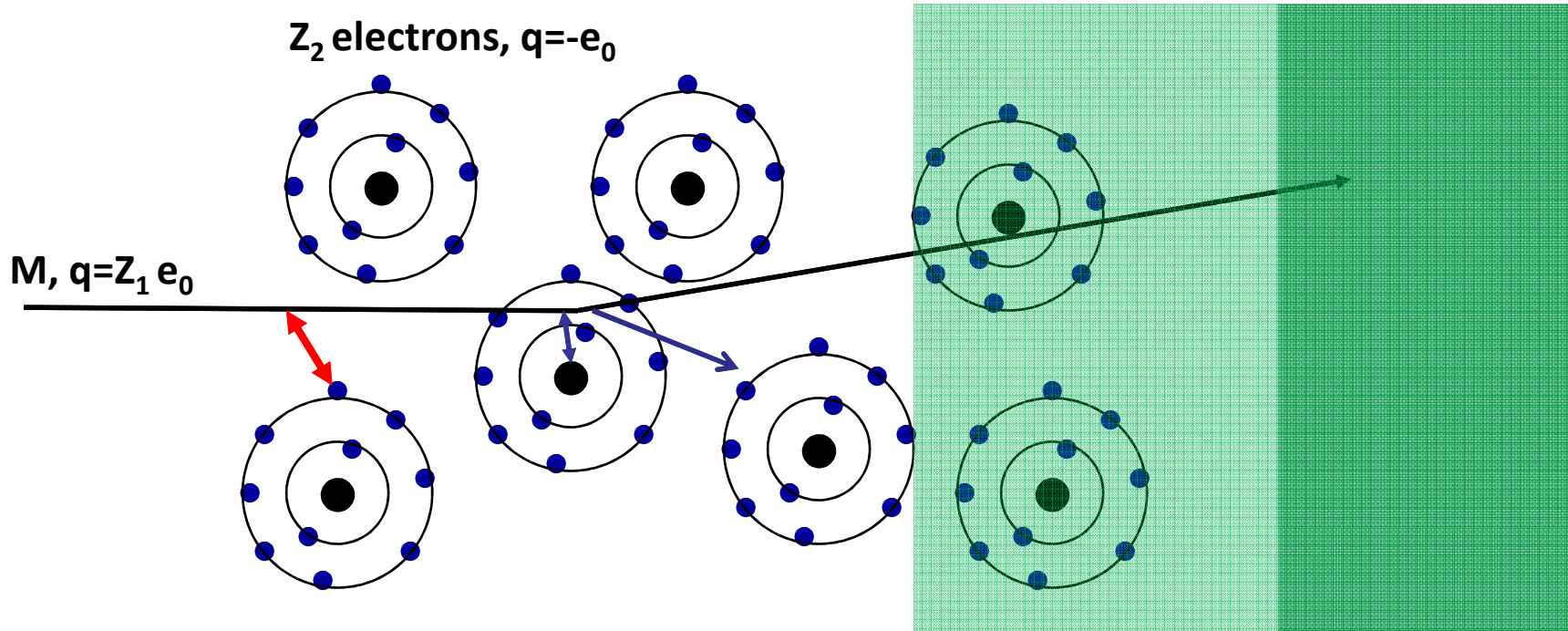


Particle Detectors

Summer Student Lectures 2009
Werner Riegler, CERN, werner.riegler@cern.ch

- ◆ **History of Instrumentation ↔ History of Particle Physics**
- ◆ **The 'Real' World of Particles**
- ◆ **Interaction of Particles with Matter**
- ◆ **Tracking with Gas and Solid State Detectors**
- ◆ **Calorimetry, Particle ID, Detector Systems**

Electromagnetic Interaction of Particles with Matter



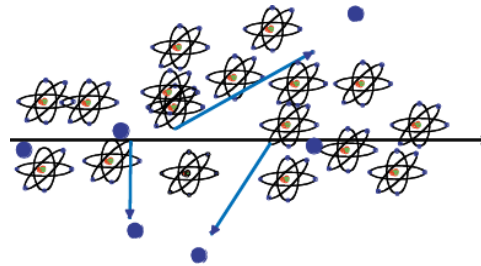
Interaction with the atomic electrons. The incoming particle loses energy and the atoms are excited or ionized.

Interaction with the atomic nucleus. The particle is deflected (scattered) causing multiple scattering of the particle in the material. During this scattering a Bremsstrahlung photon can be emitted.

In case the particle's velocity is larger than the velocity of light in the medium, the resulting EM shockwave manifests itself as Cherenkov Radiation. When the particle crosses the boundary between two media, there is a probability of the order of 1% to produce and X ray photon, called Transition radiation.

Creation of the Signal

Charged particles traversing matter leave excited atoms, electron-ion pairs (gases) or electrons-hole pairs (solids) behind.

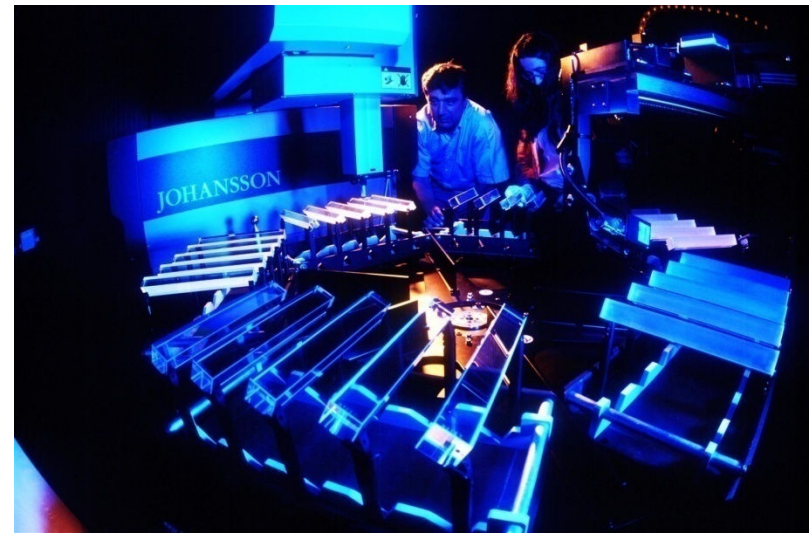
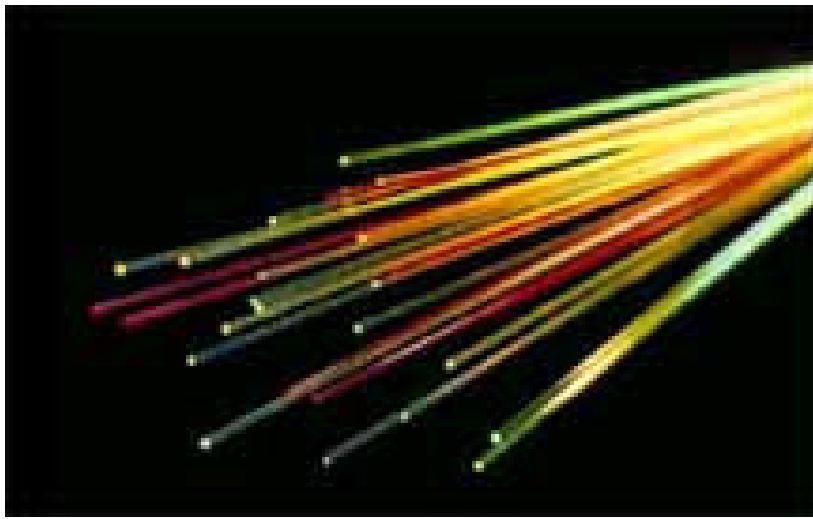


Excitation:

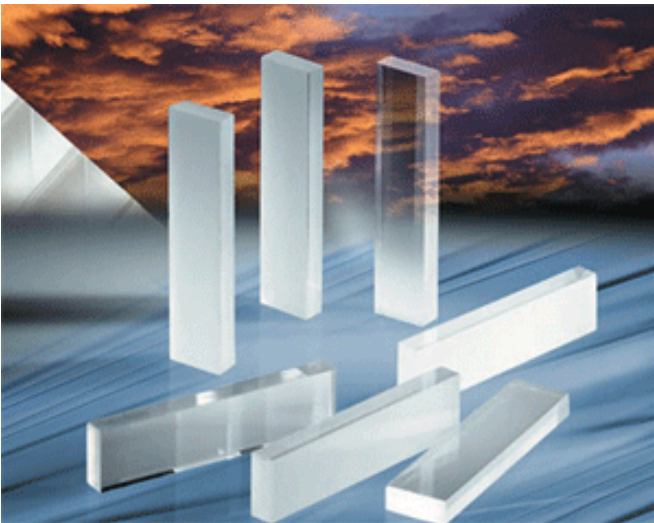
The photons emitted by the excited atoms in transparent materials can be detected with photon detectors like photomultipliers or semiconductor photon detectors.

Ionization:

By applying an electric field in the detector volume, the ionization electrons and ions are moving, which induces signals on metal electrodes. These signals are then read out by appropriate readout electronics.



Detectors based on registration of excited Atoms \rightarrow Scintillators



Detectors based on Registration of excited Atoms → Scintillators

Emission of photons of by excited Atoms, typically UV to visible light.



a) Observed in Noble Gases (even liquid !)

b) Inorganic Crystals

→ Substances with largest light yield. Used for precision measurement of energetic Photons. Used in Nuclear Medicine.

c) Polyzyclic Hydrocarbons (Naphtalen, Anthrazen, organic Scintillators)

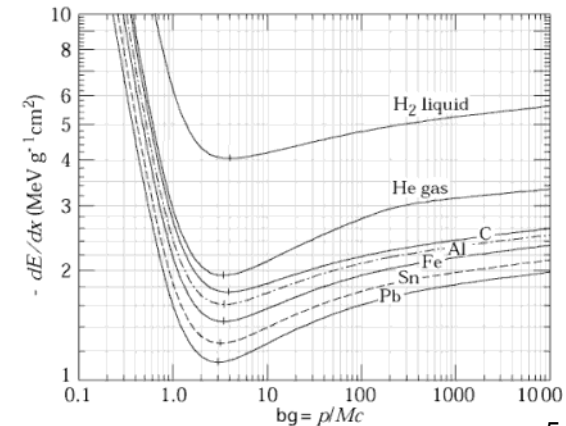
→ Most important category. Large scale industrial production, mechanically and chemically quite robust. Characteristic are one or two decay times of the light emission.

Typical light yield of scintillators:

Energy (visible photons) \approx few % of the total energy Loss.

z.B. 1cm plastic scintillator, $\rho \approx 1$, $dE/dx=1.5$ MeV, ~ 15 keV in photons;

i.e. $\sim 15\,000$ photons produced.



Detectors based on Registration of excited Atoms → Scintillators

Organic ('Plastic') Scintillators

Low Light Yield

Fast: 1-3ns

| Type | Light ^a output | λ_{\max}^a (nm) | Attenuation ^d length (cm) | Risetime (ns) | Decay ^d time (ns) | Pulse FWHM (ns) |
|---------|------------------------------|----------------------------|--|------------------|------------------------------------|-----------------------|
| NE 102A | 58-70 | 423 | 250 | 0.9 | 2.2-2.5 | 2.7-3.2 |
| NE 104 | 68 | 406 | 120 | 0.6-0.7 | 1.7-2.0 | 2.2-2.5 |
| NE 104B | 59 | 406 | 120 | 1 | 3.0 | 3 |
| NE 110 | 60 | 434 | 400 | 1.0 | 2.9-3.3 | 4.2 |
| NE 111 | 40-55 | 375 | 8 | 0.13-0.4 | 1.3-1.7 | 1.2-1.6 |
| NE 114 | 42-50 | 434 | 350-400 | ~1.0 | 4.0 | 5.3 |
| Pilot B | 60-68 | 408 | 125 | 0.7 | 1.6-1.9 | 2.4-2.7 |
| Pilot F | 64 | 425 | 300 | 0.9 | 2.1 | 3.0-3.3 |
| Pilot U | 58-67 | 391 | 100-140 | 0.5 | 1.4-1.5 | 1.2-1.9 |
| BC 404 | 68 | 408 | — | 0.7 | 1.8 | 2.2 |
| BC 408 | 64 | 425 | — | 0.9 | 2.1 | ~2.5 |
| BC 420 | 64 | 391 | — | 0.5 | 1.5 | 1.3 |
| ND 100 | 60 | 434 | 400 | — | 3.3 | 3.3 |
| ND 120 | 65 | 423 | 250 | — | 2.4 | 2.7 |
| ND 160 | 68 | 408 | 125 | — | 1.8 | 2.7 |

LHC bunchcrossing 25ns

Inorganic (Crystal) Scintillators

Large Light Yield

Slow: few 100ns

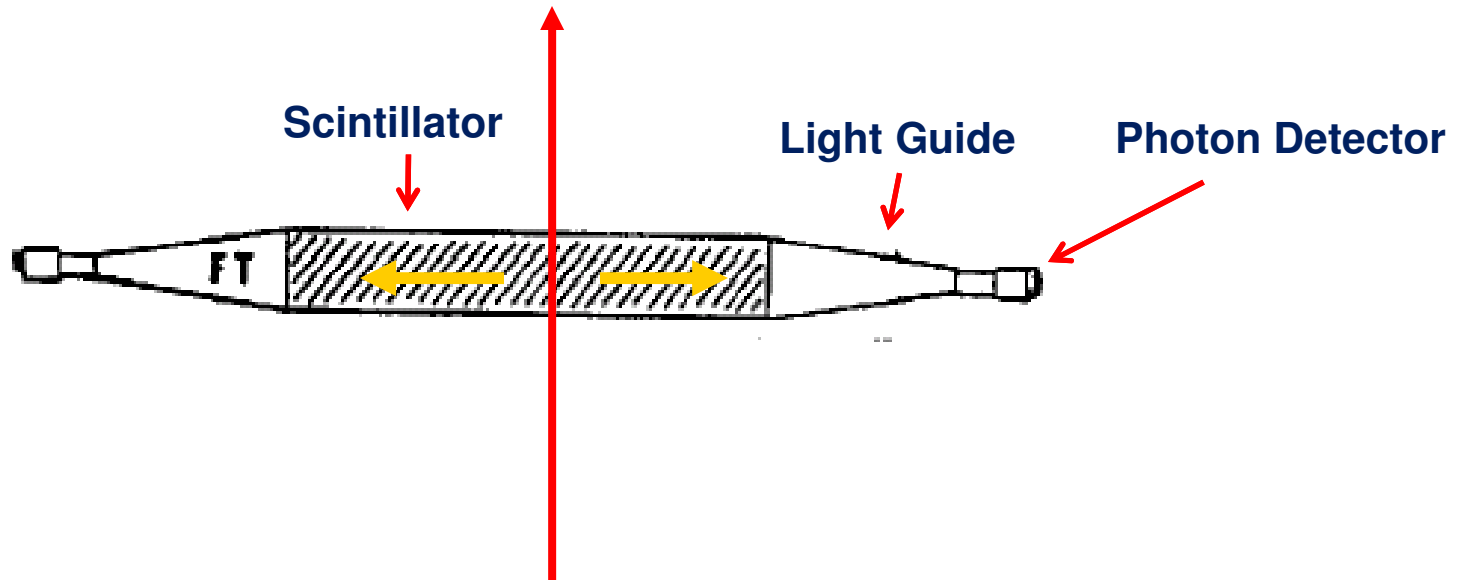
| | Relative light output | λ_{\max} emission (nm) | Decay time (ns) | Density (g/cm ³) |
|--|-----------------------------|--------------------------------------|-----------------------|---------------------------------|
| <i>Inorganic crystals</i> | | | | |
| Nal(Tl) | 230 | 415 | 230 | 3.67 |
| CsI(Tl) | 250 | 560 | 900 | 4.51 |
| Bi ₄ Ge ₃ O ₁₂ (BGO) | 23-86 | 480 | 300 | 7.13 |
| <i>Organic crystals</i> | | | | |
| Anthracene | 100 | 448 | 22 | 1.25 |
| Trans-stilbene | 75 | 384 | 4.5 | 1.16 |
| Naphthalene | 32 | 330-348 | 76-96 | 1.03 |
| <i>p,p'</i> -Quaterphenyl | 94 | 437 | 7.5 | 1.20 |
| <i>Primary activators</i> | | | | |
| 2,5-Diphenyl-oxazole (PPO) | 75 | 360-416 | 5* | |
| 2-Phenyl-5-(4-biphenyl)- 1,3,4-oxadiazole (PBD) | 96 | 360-5 | | |
| 4,4'-Bis(2-butyl-octyloxy)- <i>p</i> - quaterphenyl (BIBUQ) | 60 | 365,393 | 1.30* | |

LEP bunchcrossing 25μs

Scintillators

Photons are being reflected towards the ends of the scintillator.

A light guide brings the photons to the Photomultipliers where the photons are converted to an electrical signal.

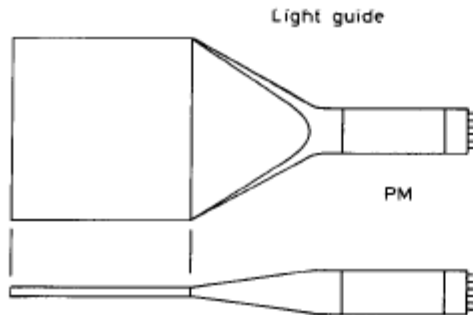


By segmentation one can arrive at spatial resolution.

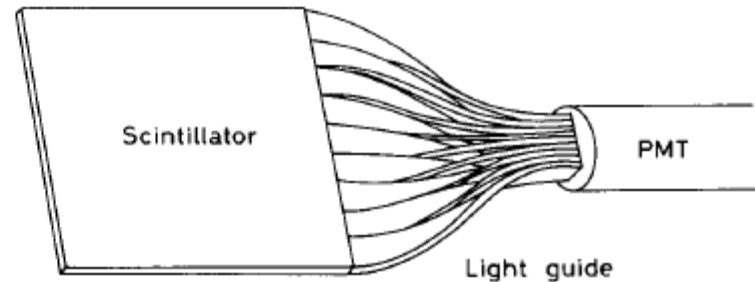
Because of the excellent timing properties ($<1\text{ns}$) the arrival time, or time of flight, can be measured very accurately \rightarrow Trigger, Time of Flight.

Typical Geometries:

- Light guides: transfer by total internal reflection (+outer reflector)



“fish tail”



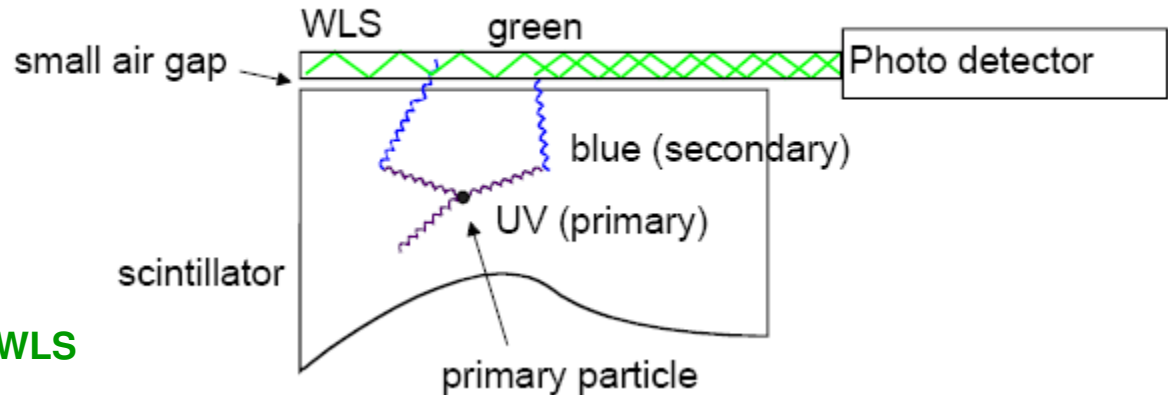
adiabatic

- wavelength shifter (WLS) bars

UV light enters the WLS material
Light is transformed into longer wavelength

→ Total internal reflection inside the WLS material

→ ‘transport’ of the light to the photo detector

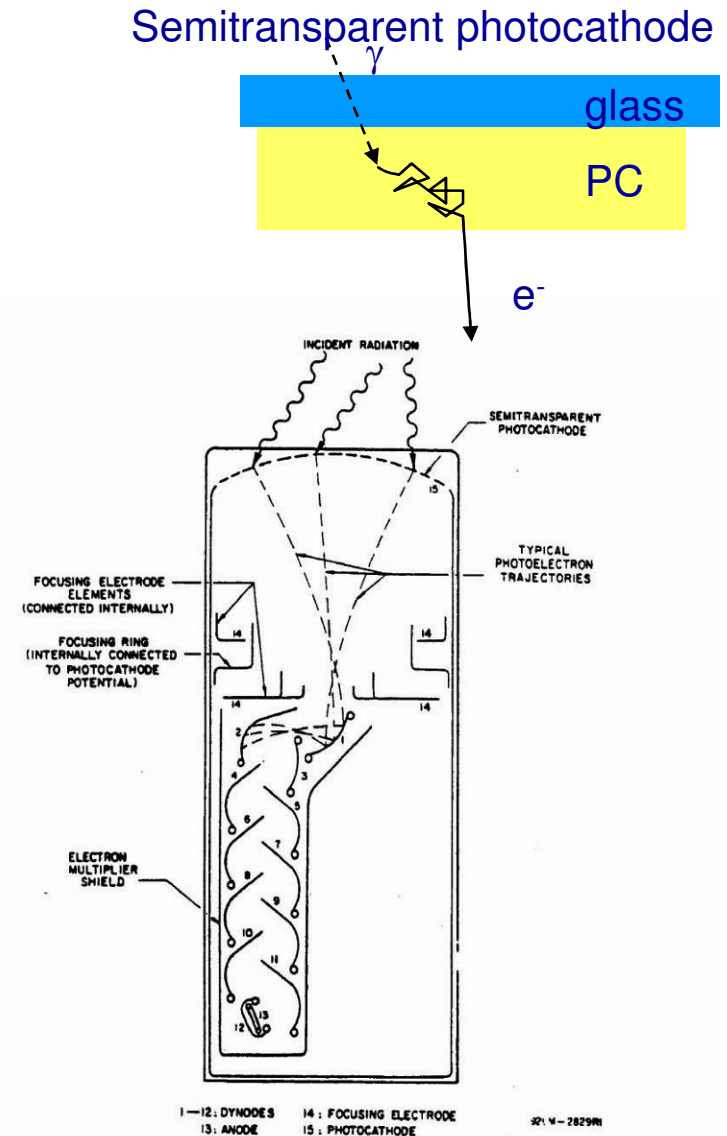


The frequent use of Scintillators is due to:

Well established and cheap techniques to register Photons → Photomultipliers
and the fast response time → 1 to 100ns

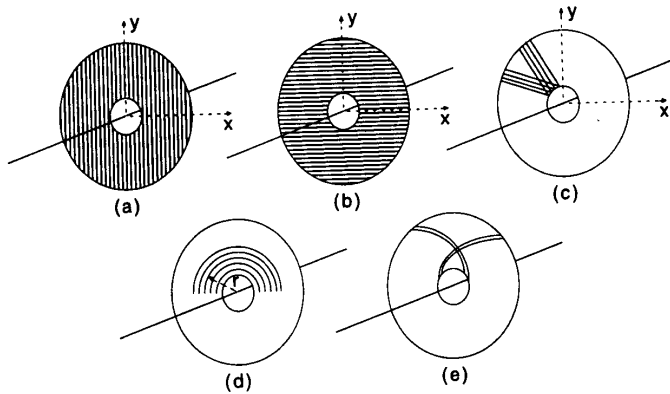
Schematic of a Photomultiplier:

- Typical Gains (as a function of the applied voltage): 10^8 to 10^{10}
- Typical efficiency for photon detection:
 - < 20%
- For very good PMs: registration of single photons possible.
- Example: 10 primary Elektrons, Gain $10^7 \rightarrow 10^8$ electrons in the end in $T \approx 10\text{ns}$. $I = Q/T = 10^8 \cdot 1.603 \cdot 10^{-19} / 10 \cdot 10^{-9} = 1.6\text{mA}$.
- Across a $50\ \Omega$ Resistor $\rightarrow U = R \cdot I = 80\text{mV}$.

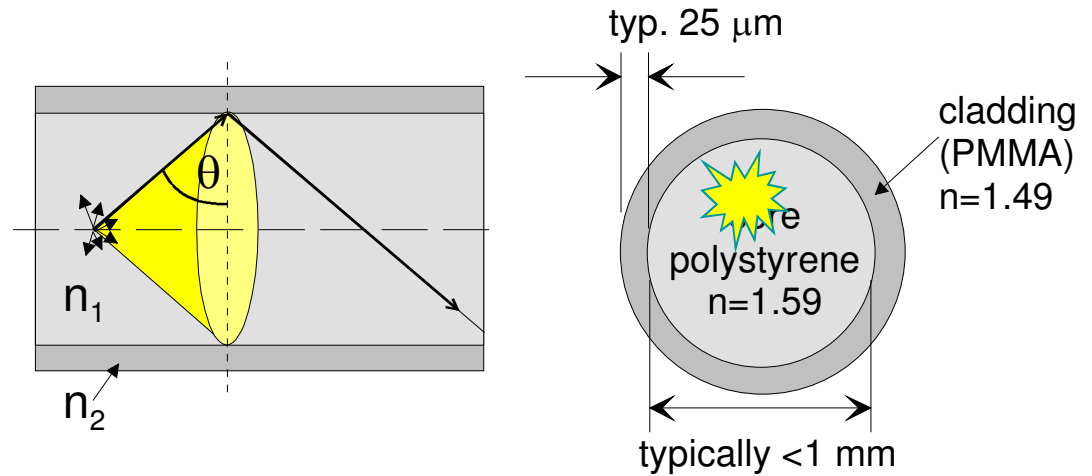


Fiber Tracking

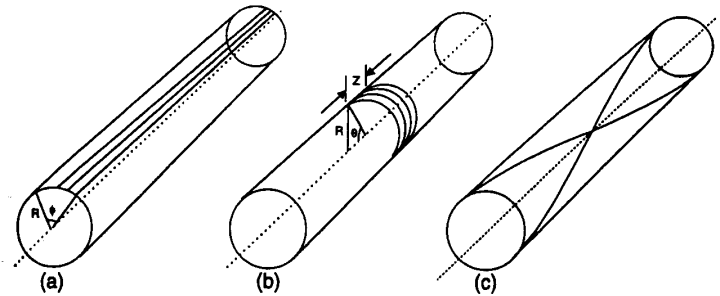
Planar geometries (end cap)



Light transport by total internal reflection



Circular geometries (barrel)



High geometrical flexibility

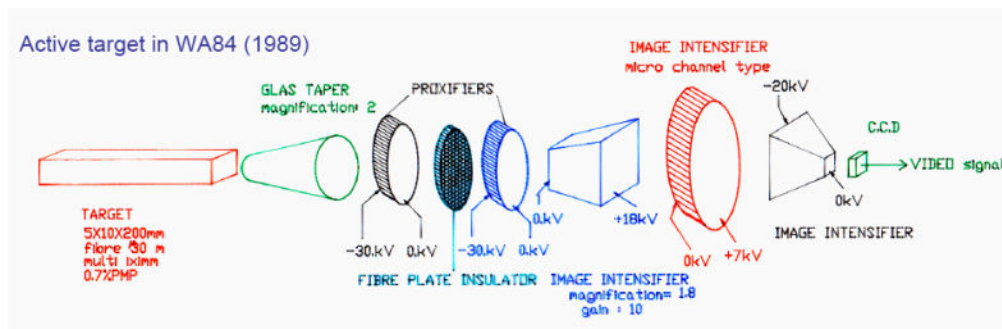
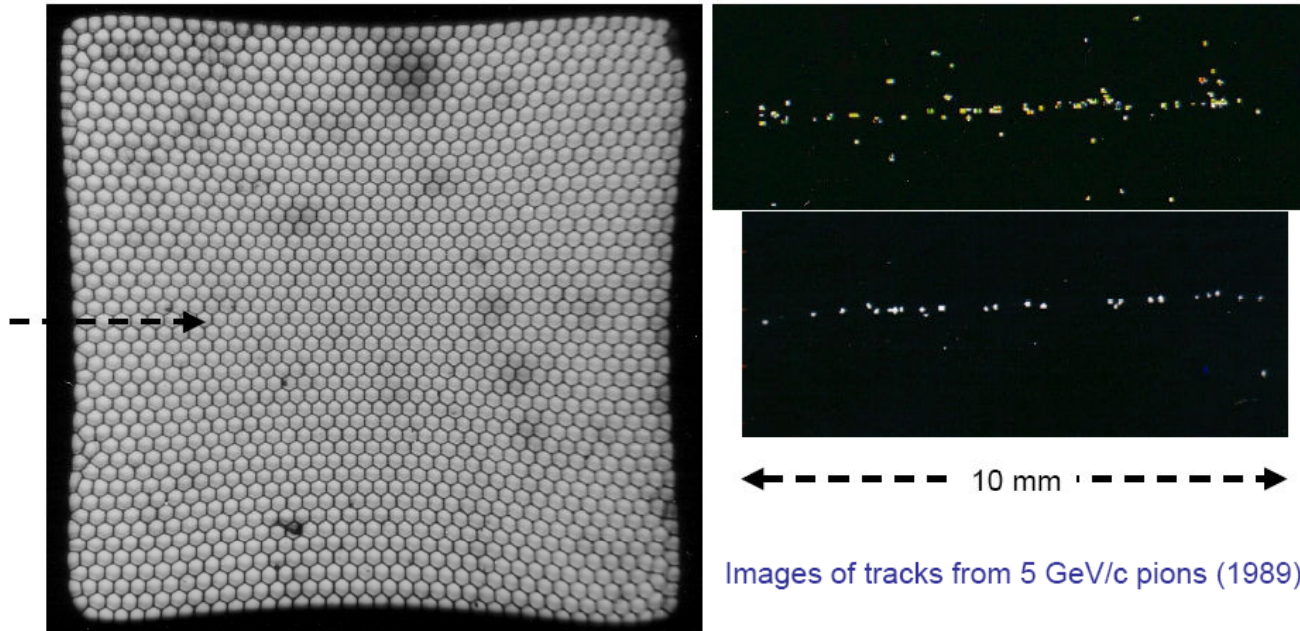
Fine granularity

Low mass

Fast response (ns)

(R.C. Ruchti, Annu. Rev. Nucl. Sci. 1996, 46,281)

Fiber Tracking



Readout of photons in a cost effective way is rather challenging.

Detectors based on Registration of Ionization: Tracking in Gas and Solid State Detectors

Charged particles leave a trail of ions (and excited atoms) along their path: Electron-Ion pairs in gases and liquids, electron hole pairs in solids.

The produced charges can be registered → Position measurement → Tracking Detectors.

Cloud Chamber: Charges create drops → photography.

Bubble Chamber: Charges create bubbles → photography.

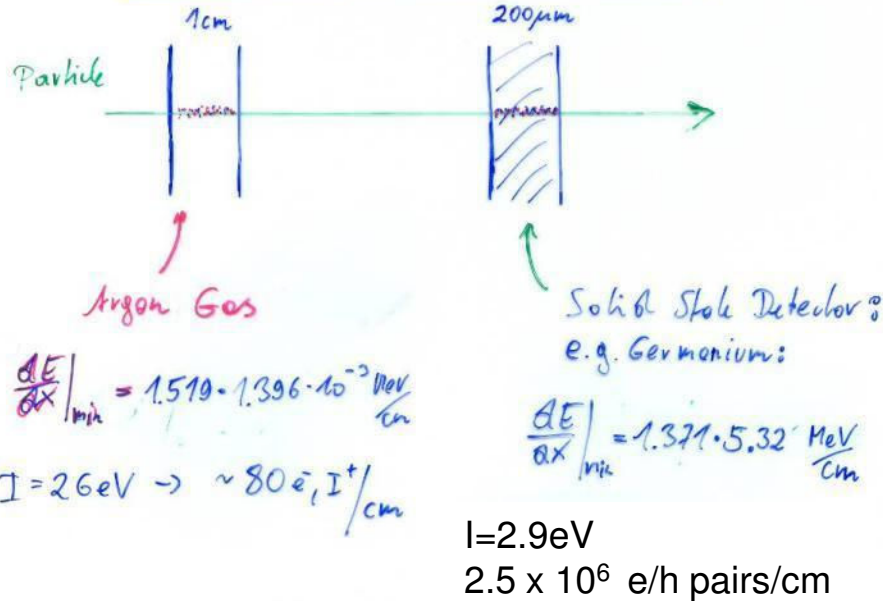
Emulsion: Charges 'blackened' the film.

Gas and Solid State Detectors: Moving Charges (electric fields) induce electronic signals on metallic electrodes that can be read by dedicated electronics.

→ In solid state detectors the charge created by the incoming particle is sufficient.

→ In gas detectors (e.g. wire chamber) the charges are internally multiplied in order to provide a measurable signal.

Gas Detectors, Solid State Detectors



The induced signals are readout out by dedicated electronics.

The noise of an amplifier determines whether the signal can be registered. Signal/Noise $\gg 1$

The noise is characterized by the 'Equivalent Noise Charge (ENC)' = Charge signal at the input that produced an output signal equal to the noise.

ENC of very good amplifiers can be as low as 50e-, typical numbers are $\sim 1000e^-$.

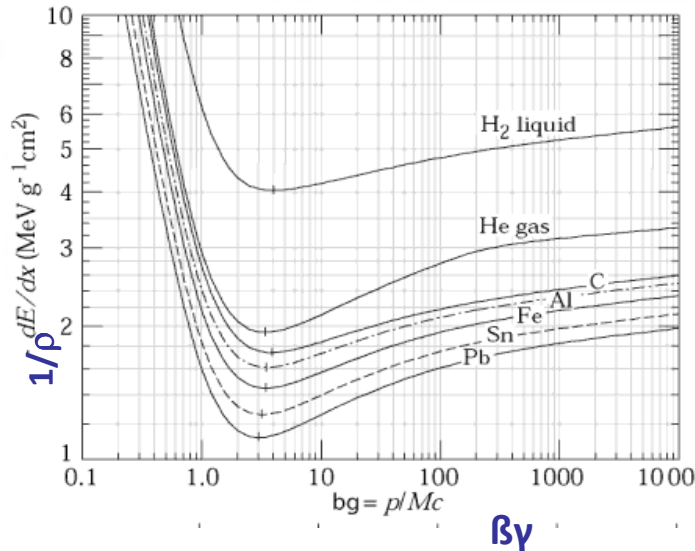
In order to register a signal, the registered charge must be $q \gg \text{ENC}$ i.e. typically $q \gg 1000e^-$.

Gas Detector: $q = 80e^- / cm \rightarrow$ too small.

Solid state detectors have 1000x more density and factor 5-10 less ionization energy.
 \rightarrow Primary charge is 10^4 - 10^5 times larger than is gases.

Gas detectors need internal amplification in order to be sensitive to single particle tracks.

Without internal amplification they can only be used for a large number of particles that arrive at the same time (ionization chamber).



Principle of Signal Induction by Moving Charges

A point charge q at a distance z_0

Above a grounded metal plate
'induces' a surface charge.

The total induced charge on the
surface is $-q$.

Different positions of the charge result
in different charge distributions.
The total induced charge stays $-q$.

The electric field of the charge must be
calculated with the boundary condition
that the potential $\phi=0$ at $z=0$.

For this specific geometry the method of
images can be used. A point charge $-q$ at
distance $-z_0$ satisfies the boundary
condition \rightarrow electric field.

● q

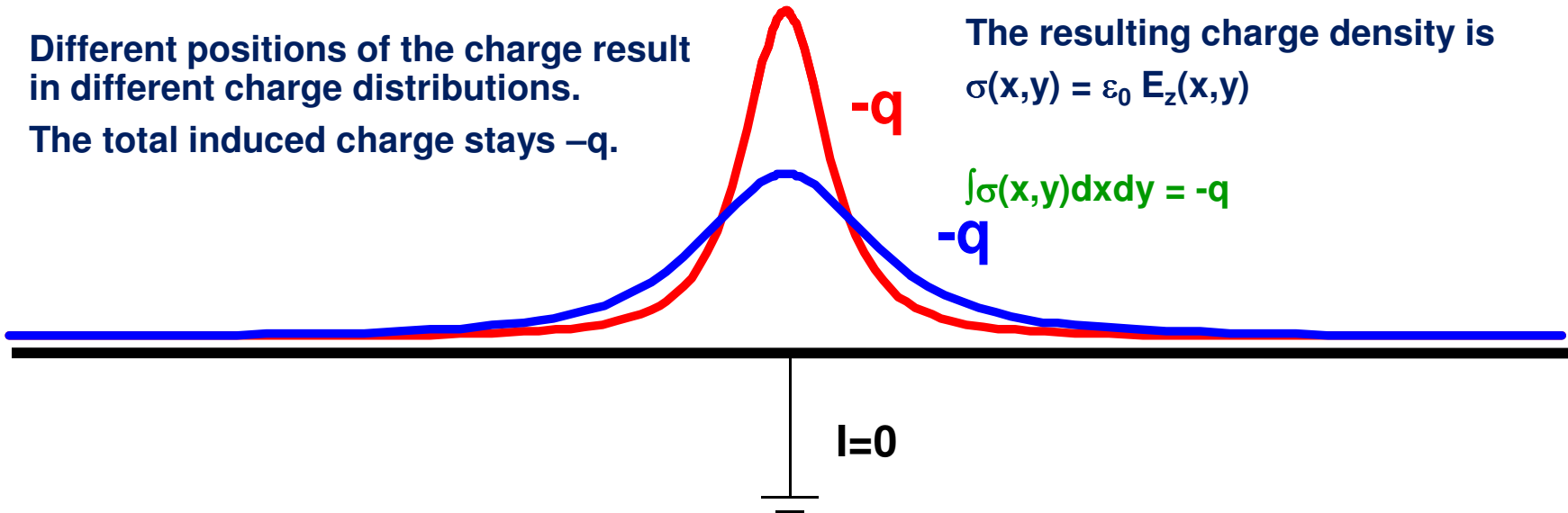
● q

$-q$

$-q$

The resulting charge density is
 $\sigma(x,y) = \epsilon_0 E_z(x,y)$

$$\int \sigma(x,y) dx dy = -q$$



$$E_z(x,y) = -\frac{qz_0}{2\pi\epsilon_0(x^2 + y^2 + z_0^2)^{\frac{3}{2}}}$$

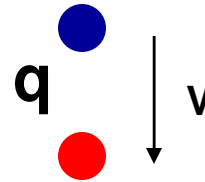
$$E_x = E_y = 0$$

$$\sigma(x,y) = \epsilon_0 E_z(x,y)$$

$$Q = \int_{-\infty}^{\infty} \int_{-\infty}^{\infty} \sigma(x,y) dx dy = -q$$

Principle of Signal Induction by Moving Charges

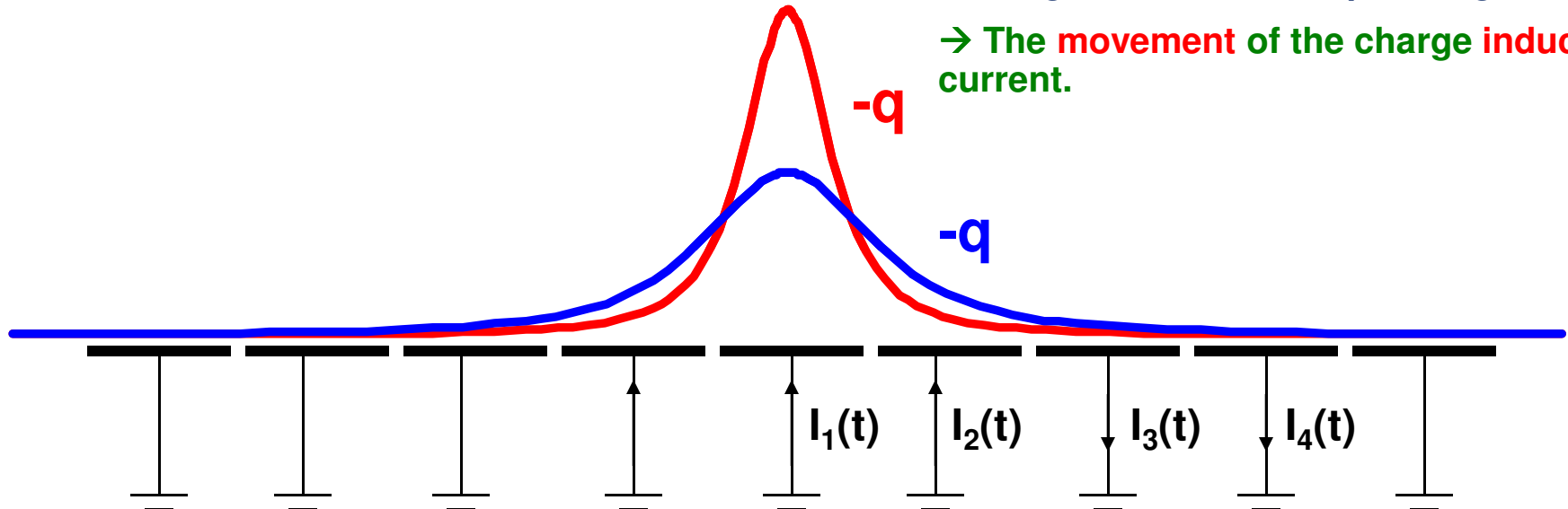
If we segment the grounded metal plate and if we ground the individual strips the surface charge density doesn't change with respect to the continuous metal plate.



The charge induced on the individual strips is now depending on the position z_0 of the charge.

If the charge is moving there are currents flowing between the strips and ground.

→ The movement of the charge induces a current.



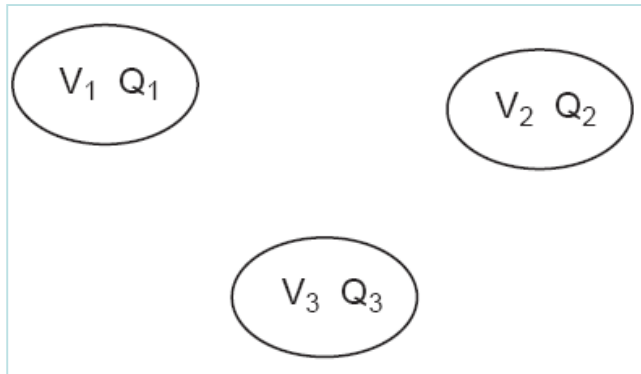
$$Q_1(z_0) = \int_{-\infty}^{\infty} \int_{-w/2}^{w/2} \sigma(x, y) dx dy = -\frac{2q}{\pi} \arctan\left(\frac{w}{2z_0}\right)$$

$$z_0(t) = z_0 - vt$$

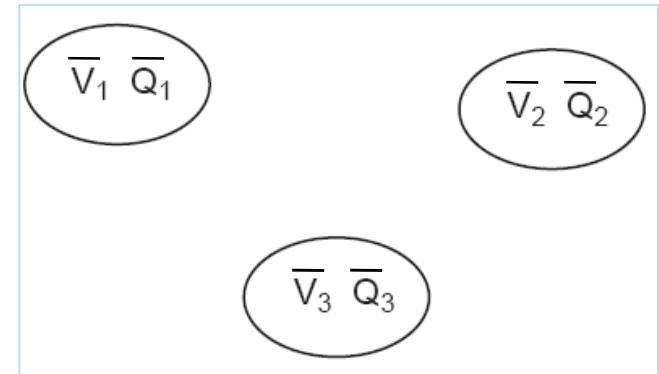
$$I_1^{ind}(t) = -\frac{d}{dt} Q_1[z_0(t)] = -\frac{\partial Q_1[z_0(t)]}{\partial z_0} \frac{dz_0(t)}{dt} = \frac{4qw}{\pi[4z_0(t)^2 + w^2]} v$$

Signal Theorems

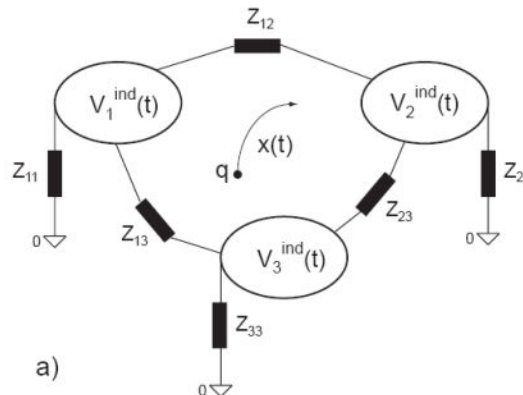
Placing charges on metal electrodes results in certain potentials of these electrodes. A different set of charges results in a different set of potentials. The reciprocity theorem states that



$$\sum_{n=1}^N Q_n \bar{V}_n = \sum_{n=1}^N \bar{Q}_n V_n$$



Using this theorem we can answer the following general question: What are the signals created by a moving charge on metal electrodes that are connected with arbitrary discrete (linear) components ?



12/3/2009

Signal Theorems

What are the charges induced by a moving charge on electrodes that are connected with arbitrary linear impedance elements ?

One first removes all the impedance elements, connects the electrodes to ground and calculates the currents induced by the moving charge on the grounded electrodes.

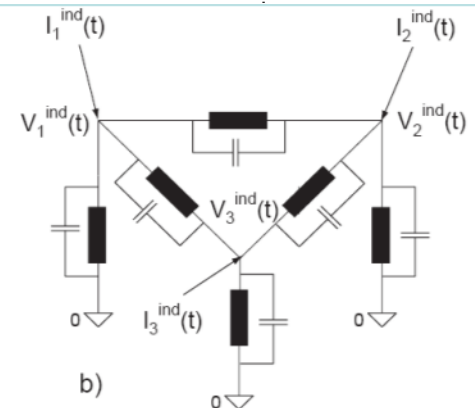
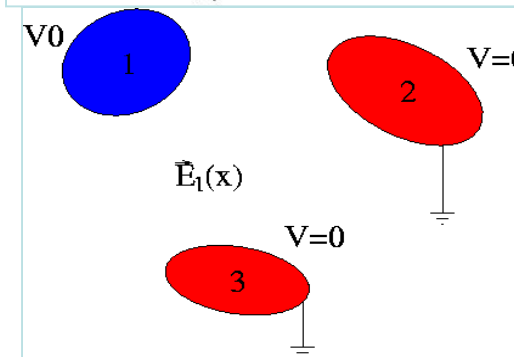
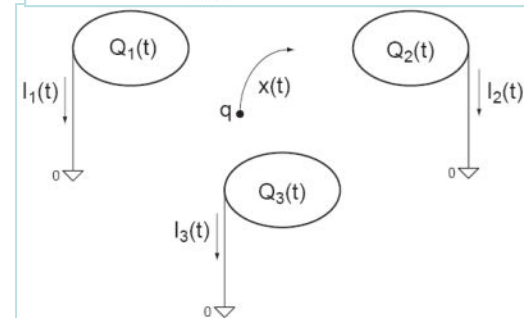
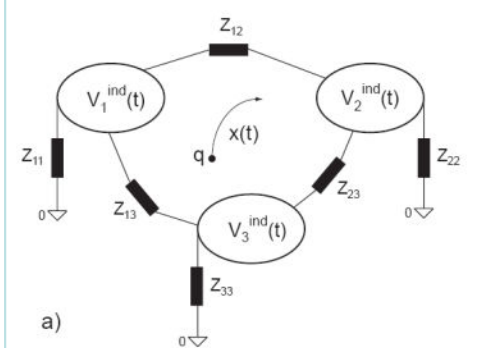
The current induced on a grounded electrode by a charge q moving along a trajectory $x(t)$ is calculated the following way (Ramo Theorem):

One removes the charge q from the setup, puts the electrode to voltage V_0 while keeping all other electrodes grounded. This results in an electric field $E_n(x)$, the Weighting Field, in the volume between the electrodes, from which the current is calculated by

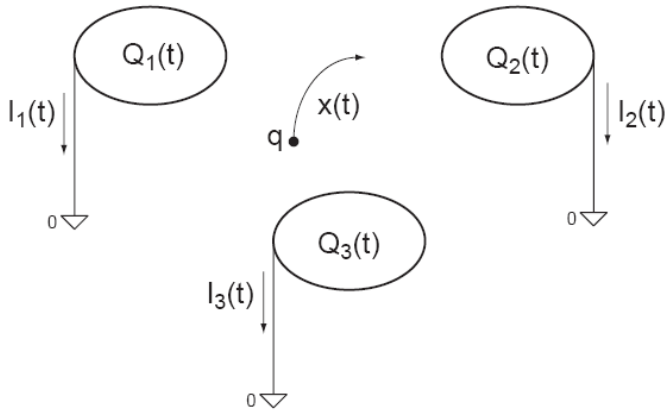
$$I_n(t) = -\frac{q}{V_0} \vec{E}_n[\vec{x}(t)] \frac{d\vec{x}(t)}{dt} = -\frac{q}{V_0} \vec{E}_n[\vec{x}(t)] \vec{v}(t)$$

These currents are then placed as ideal current sources on a circuit where the electrodes are 'shrunk' to simple nodes and the mutual electrode capacitances are added between the nodes. These capacitances are calculated from the weighting fields by

$$c_{nm} = \frac{\varepsilon_0}{V_w} \oint_{A_n} \vec{E}_m(x) d\vec{A} \quad C_{nn} = \sum_m c_{nm} \quad C_{nm} = -c_{nm} \quad n \neq m$$



Signal Theorems

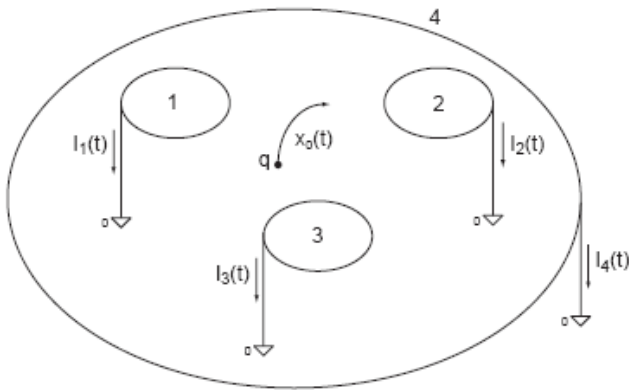


The following relations hold for the induced currents:

- 1) The charge induced on an electrode in case a charge in between the electrode has moved from a point x_0 to a point x_1 is

$$Q_n^{ind} = \int_{t_0}^{t_1} I_n^{ind}(t) dt = -\frac{q}{V_w} \int_{t_0}^{t_1} \mathbf{E}_n[\mathbf{x}(t)] \dot{\mathbf{x}}(t) dt = \frac{q}{V_w} [\psi_n(\mathbf{x}_1) - \psi_n(\mathbf{x}_0)]$$

and is independent on the actual path.

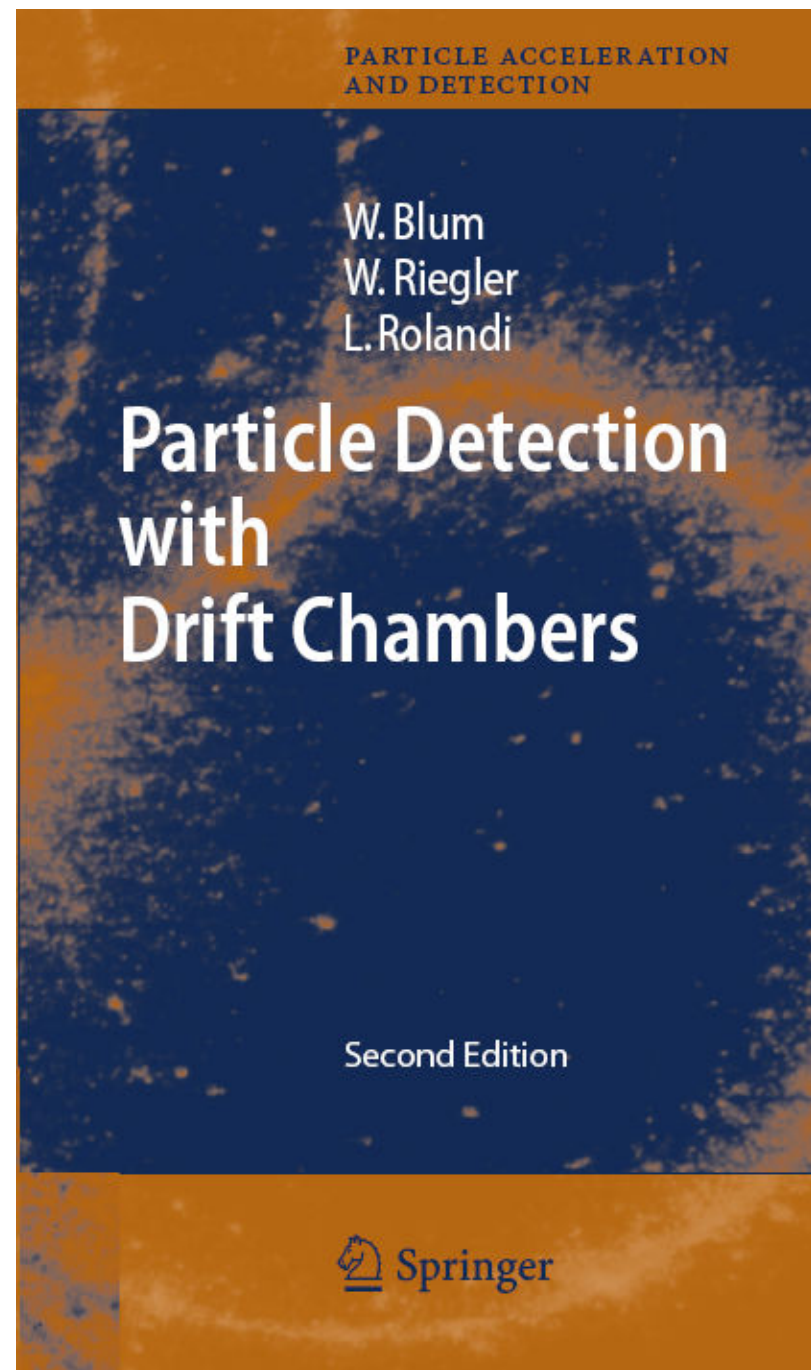


- 2) Once ALL charges have arrived at the electrodes, the total induced charge in the electrodes is equal to the charge that has ARRIVED at this electrode.

- 3) In case there is one electrode enclosing all the others, the sum of all induced currents is zero at any time.

12/3/2009

More on signal theorems, readout electronics etc. can be found in this book →



Signals in a Parallel Plate Geometry

E.g.: Elektron-ion pair in gas
 or Electron-ion pair in a liquid
 or Electron-hole pair in a solid

$$E_1 = V_0/D$$

$$E_2 = -V_0/D$$

$$I_1 = -(-q)/V_0 \cdot (V_0/D) \cdot v_e - q/V_0 \cdot (V_0/D) \cdot (-v_i)$$

$$= q/D \cdot v_e + q/D \cdot v_i$$

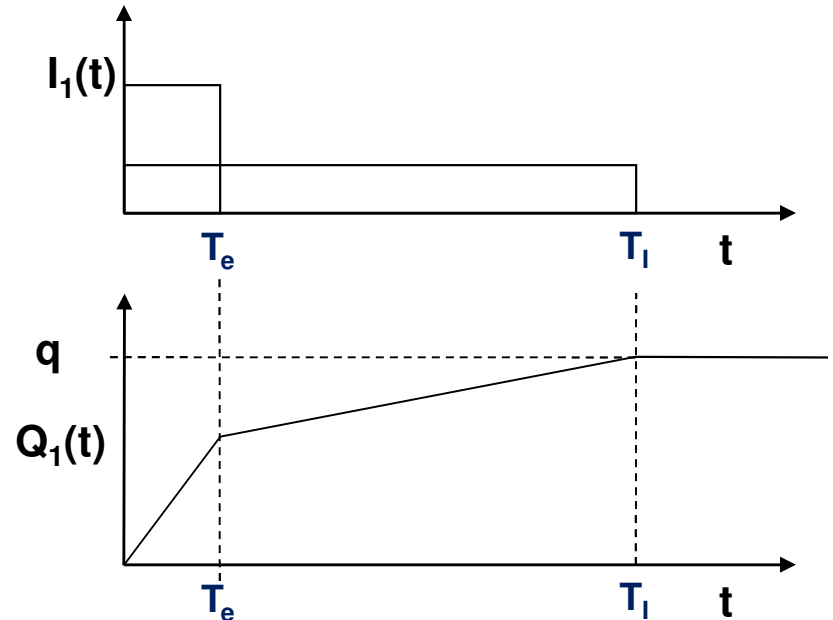
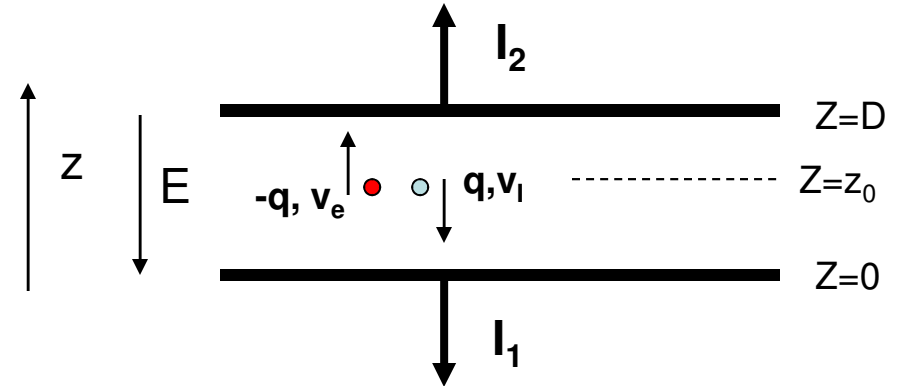
$$I_2 = -I_1$$

$$Q_1^{\text{tot}} = \int I_1 dt = q/D \cdot v_e T_e + q/D \cdot v_i T_i$$

$$= q/D \cdot v_e \cdot (D - z_0)/v_e + q/D \cdot v_i \cdot z_0/v_i$$

$$= q(D - z_0)/D + qz_0/D =$$

$$q_e + q_i = q$$



The total induced charge on a specific electrode, once all the charges have arrived at the electrodes, is equal to the charge that has arrived at this specific electrode.

Detectors based on Ionization

→ Gas detectors:

- Wire Chambers
- Drift Chambers
- Time Projection Chambers
- Transport of Electrons and Ions in Gases

Solid State Detectors

- Transport of Electrons and Holes in Solids
- Si- Detectors
- Diamond Detectors

Gas Detectors with internal Electron Multiplication

Principle: At sufficiently high electric fields (100kV/cm) the electrons gain energy in excess of the ionization energy → secondary ionization etc. etc.

$$dN = N \alpha dx$$

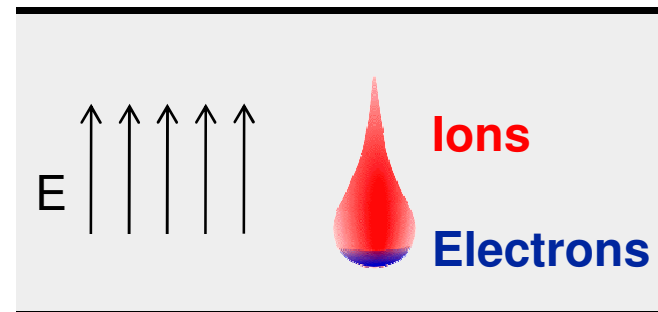
α ...Townsend Coefficient

$$N(x) = N_0 \exp(\alpha x)$$

$$N / N_0 = A \text{ (Amplification, Gas Gain)}$$

Avalanche in a homogeneous field:

Problem: High field on electrode surface
→ breakdown



In an inhomogeneous Field: $\alpha(E) \rightarrow N(x) = N_0 \exp [\int \alpha(E(x')) dx']$

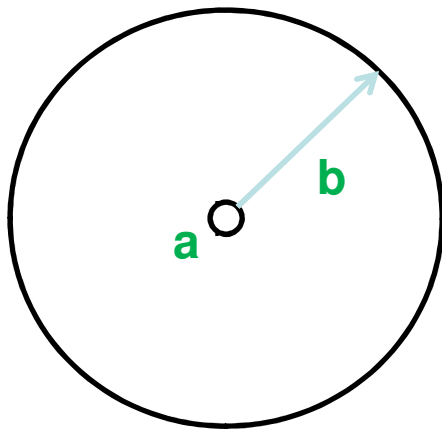
Wire Chamber: Electron Avalanche

Wire with radius (10-25 μm) in a tube of radius b (1-3cm):

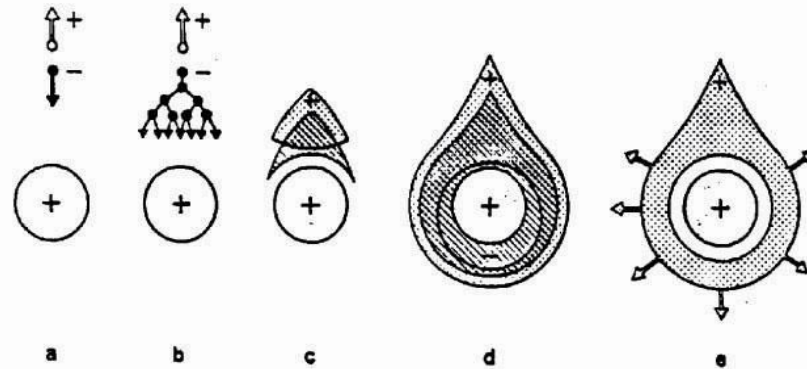
$$E(r) = \frac{\lambda}{2\pi\epsilon_0 r} = \frac{V_0}{\ln \frac{b}{a}} \frac{1}{r}, \quad V(r) = \frac{V_0}{\ln \frac{b}{a}} \ln \frac{r}{a},$$

Electric field close to a thin wire (100-300kV/cm). E.g. $V_0=1000\text{V}$, $a=10\mu\text{m}$, $b=10\text{mm}$, $E(a)=150\text{kV/cm}$

Electric field is sufficient to accelerate electrons to energies which are sufficient to produce secondary ionization \rightarrow electron avalanche \rightarrow signal.



Wire



Wire Chamber: Electron Avalanches on the Wire

Proportional region: $A \approx 10^3 - 10^4$

LHC



Semi proportional region: $A \approx 10^4 - 10^5$
(space charge effect)

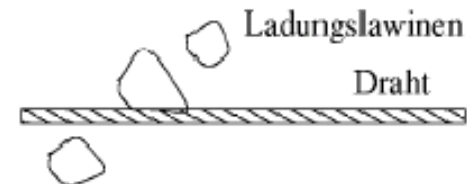


Saturation region: $A > 10^6$
Independent the number of primary electrons.

1970ies



Streamer region: $A > 10^7$
Avalanche along the particle track.

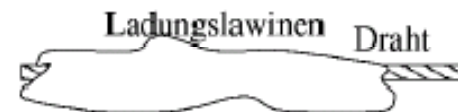


Limited Geiger region:
Avalanche propagated by UV photons.



Geiger region: $A \approx 10^9$
Avalanche along the entire wire.

1950ies

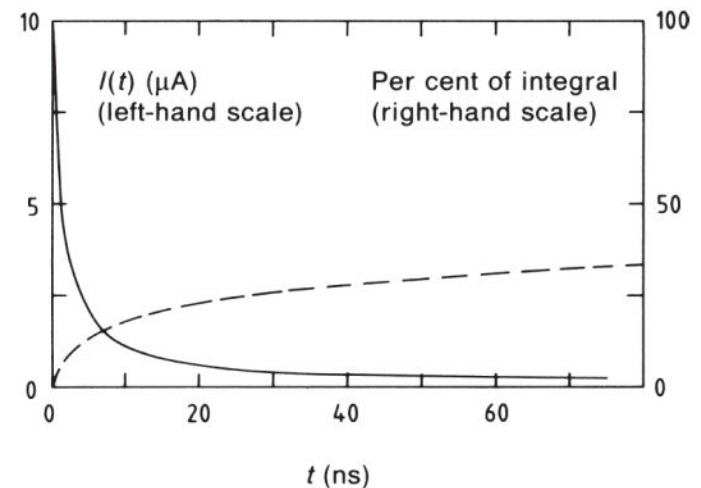
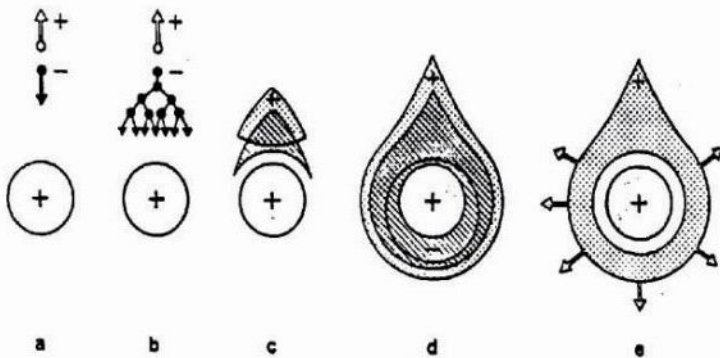


Wire Chamber: Signals from Electron Avalanches

The electron avalanche happens very close to the wire. First multiplication only around $R = 2 \times$ wire radius. Electrons are moving to the wire surface very quickly ($< 1 \text{ ns}$). Ions are drifting towards the tube wall (typically several $100 \mu\text{s}$.)

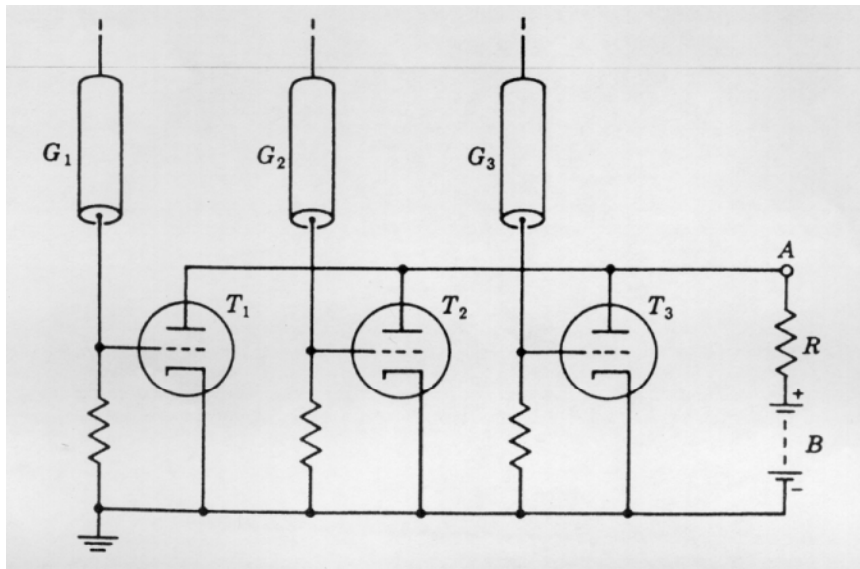
The signal is characterized by a very fast 'spike' from the electrons and a long ion tail.

The total charge induced by the electrons, i.e. the charge of the current spike due to the short electron movement amounts to 1-2% of the total induced charge.



Detectors with Electron Multiplication

Rossi 1930: Coincidence circuit for n tubes

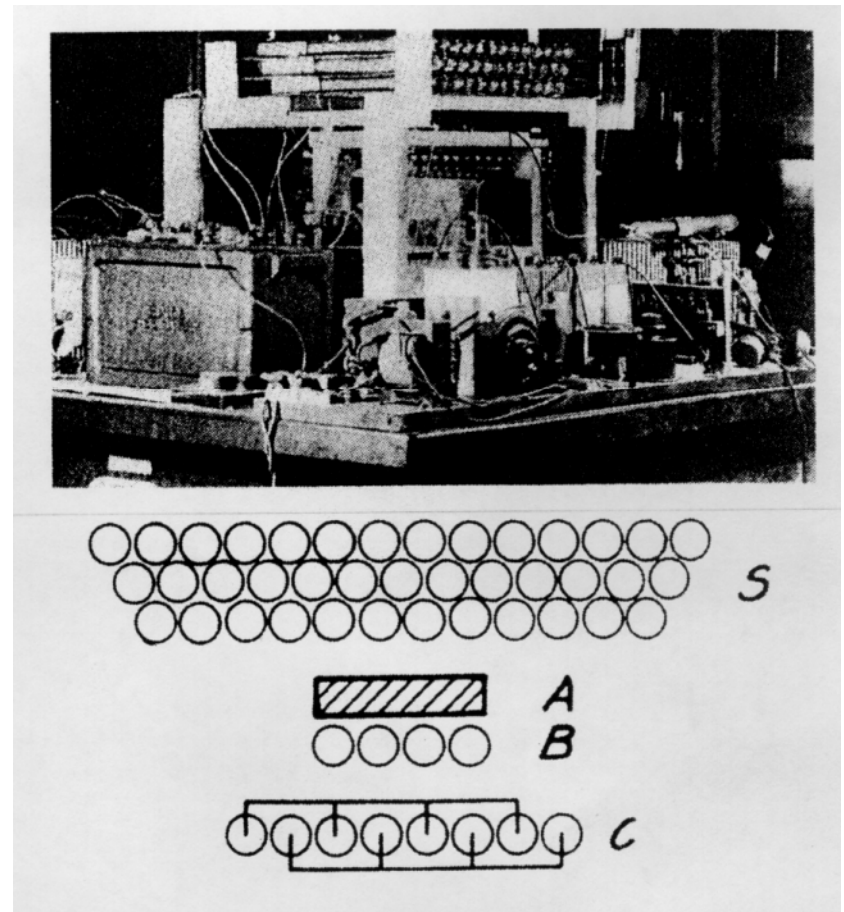


Geiger mode, large deadtime

Position resolution is determined by the size of the tubes.

Signal was directly fed into an electronic tube.

Cosmic ray telescope 1934



Multi Wire Proportional Chamber

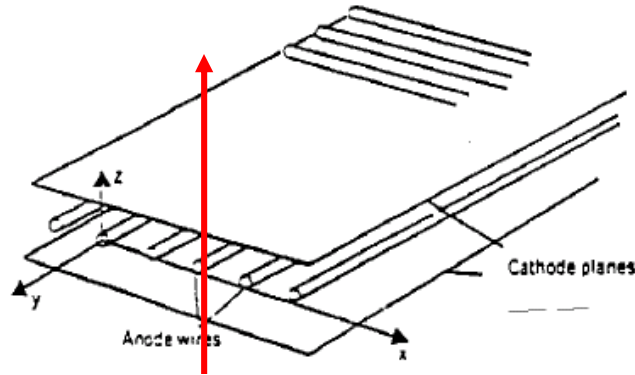
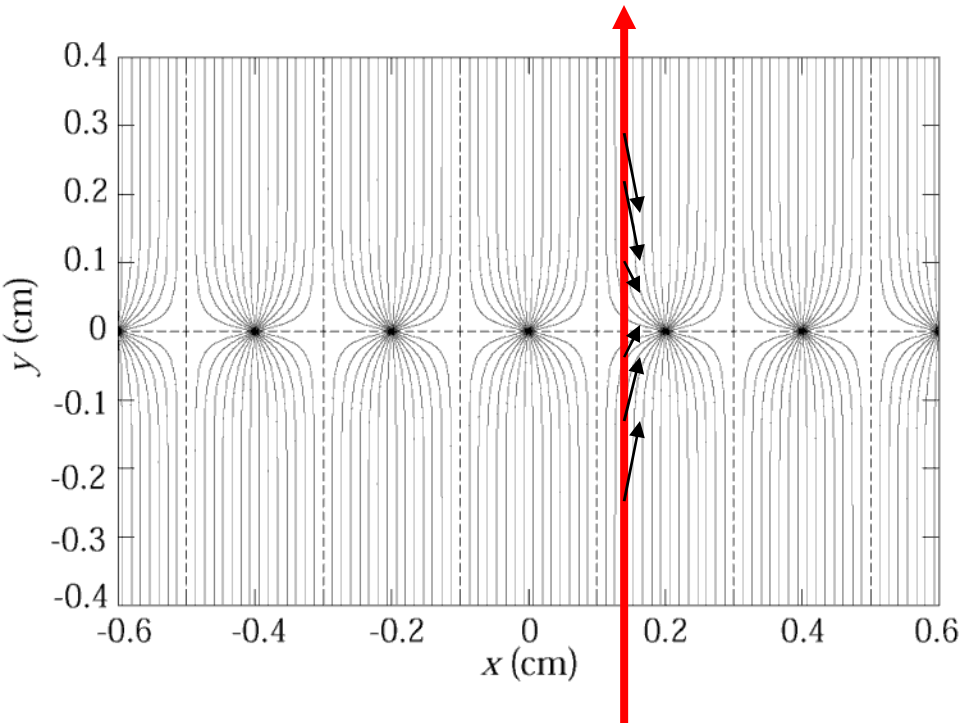


Abbildung 2.27: Vieldrahtproportionalkammer.



Classic geometry (Crossection), Charpak 1968 :

One plane of thin sense wires is placed between two parallel plates.

Typical dimensions:

Wire distance 2-5mm, distance between cathode planes ~10mm.

Electrons ($v \approx 5 \text{ cm}/\mu\text{s}$) are collected within $\approx 100 \text{ ns}$. The ion tail can be eliminated by electronics filters \rightarrow pulses of $< 100 \text{ ns}$ length.

For 10% occupancy \rightarrow every μs one pulse

\rightarrow 1MHz/wire rate capability !

\rightarrow Compare to Bubble Chamber with 10 Hz !

Multi Wire Proportional Chamber

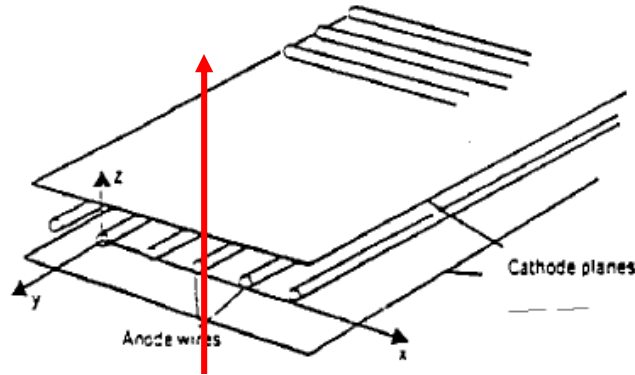
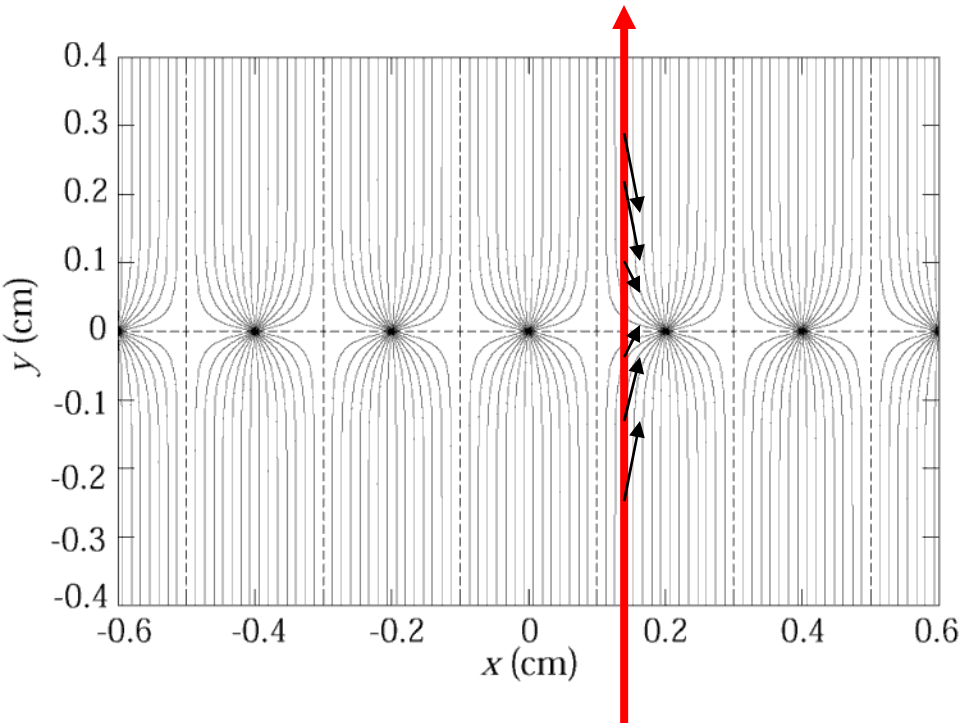


Abbildung 2.27: Vieldrahtproportionalkammer.



In order to eliminate the left/right ambiguities: Shift two wire chambers by half the wire pitch.

For second coordinate:

→ Another chamber at 90° relative rotation

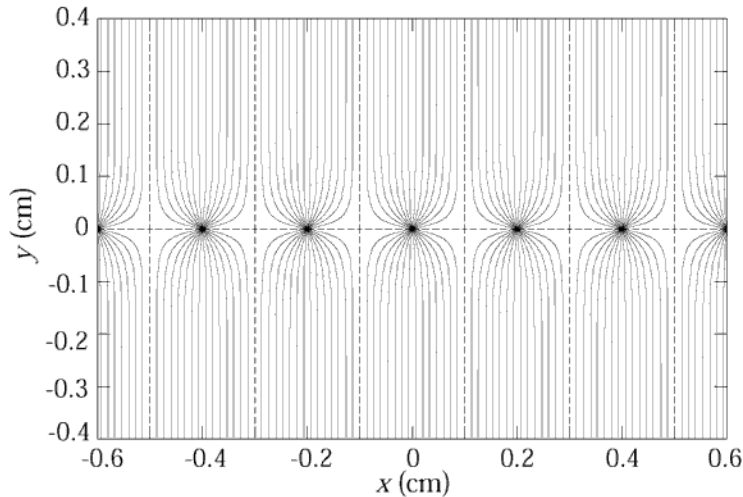
→ Signal propagation to the two ends of the wire.

→ Pulse height measurement on both ends of the wire. Because of resistivity of the wire, both ends see different charge.

Segmenting of the cathode into strips or pads:

The movement of the charges induces a signal on the wire AND on the cathode. By segmentation of the cathode plane and charge interpolation, resolutions of 50μm can be achieved.

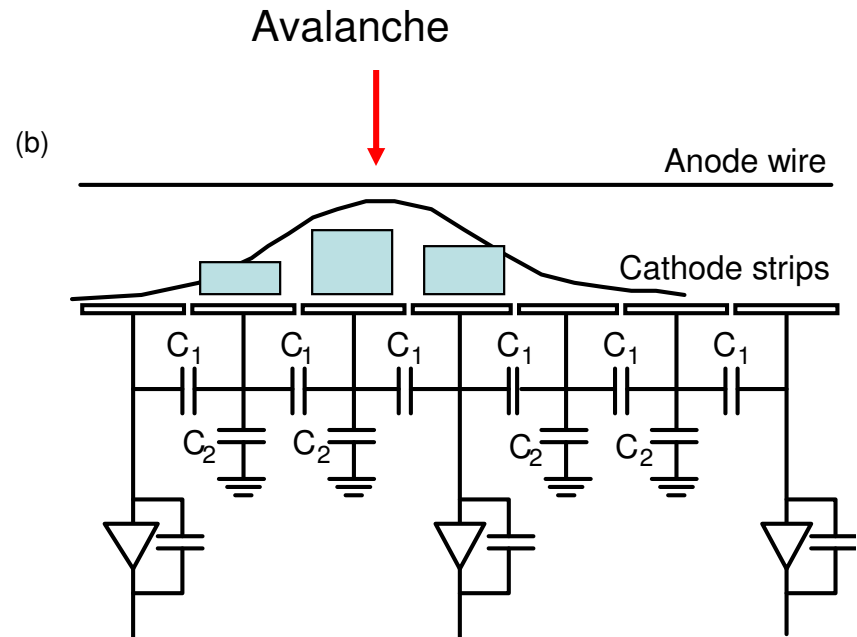
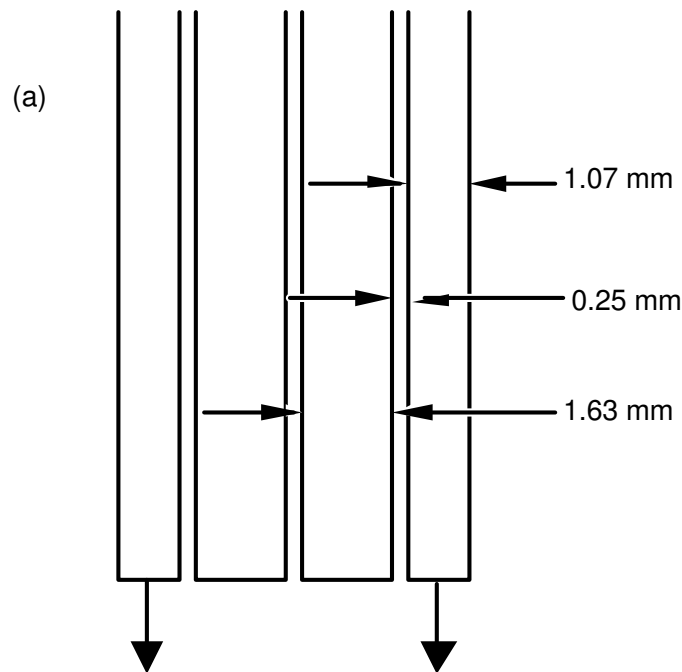
Multi Wire Proportional Chamber



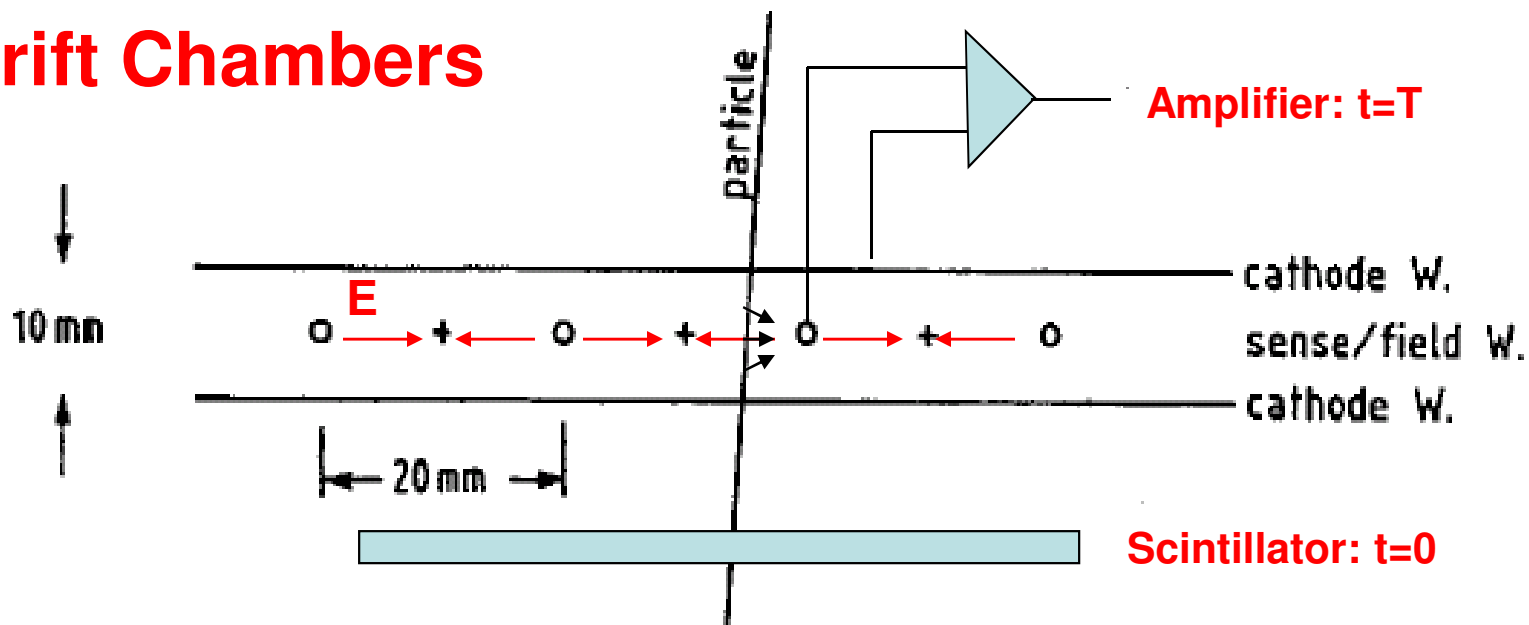
Cathode strip:

Width (1σ) of the charge distribution \approx distance between Wires and cathode plane.

‘Center of gravity’ defines the particle trajectory.



Drift Chambers



In an alternating sequence of wires with different potentials one finds an electric field between the 'sense wires' and 'field wires'.

The electrons are moving to the sense wires and produce an avalanche which induces a signal that is read out by electronics.

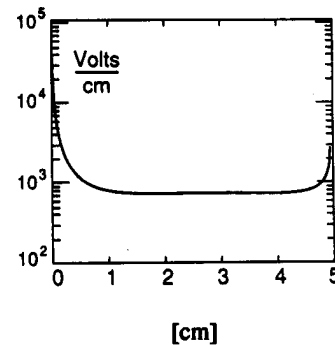
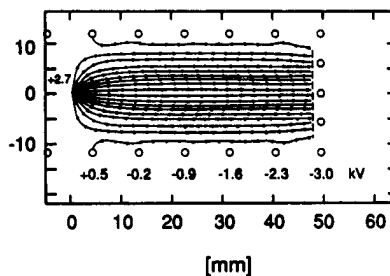
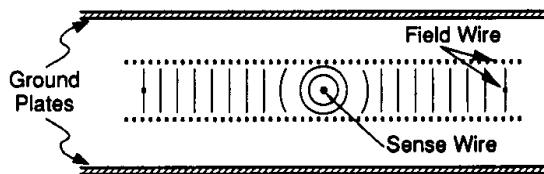
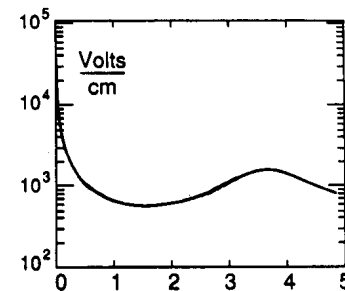
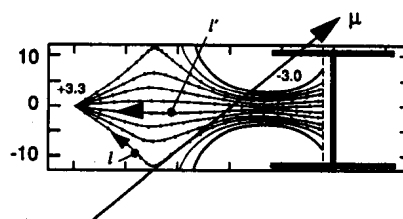
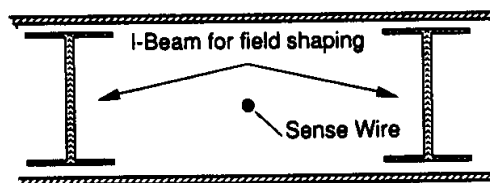
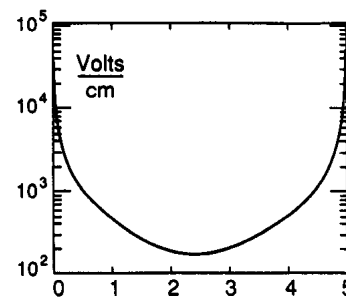
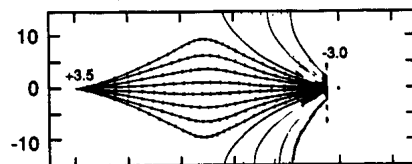
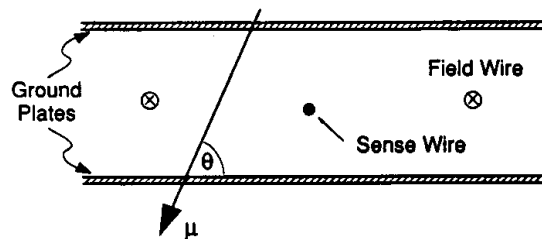
The time between the passage of the particle and the arrival of the electrons at the wire is measured.

The drift time T is a measure of the position of the particle !

By measuring the drift time, the wire distance can be increased (compared to the Multi Wire Proportional Chamber) → save electronics channels !

Drift Chambers, typical Geometries

Electric Field $\approx 1\text{kV/cm}$

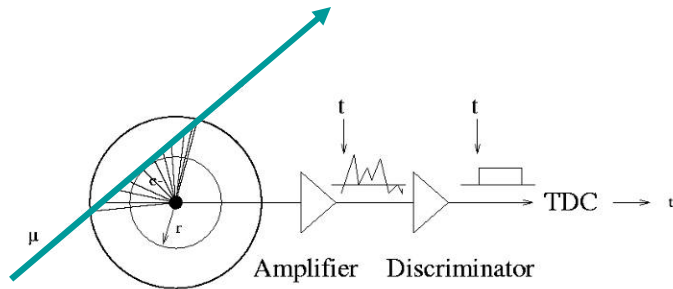


U.Becker Instr. of HEP, Vol#9, p516 World Scientific (1992) ed F.Sauli

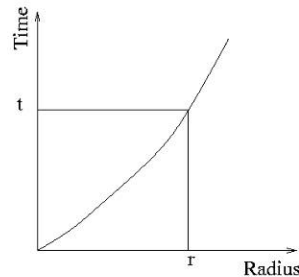
The Geiger Counter reloaded: Drift Tube

Primary electrons are drifting to the wire.

ATLAS MDT $R(\text{tube}) = 15\text{mm}$



Calibrated Radius-Time correlation

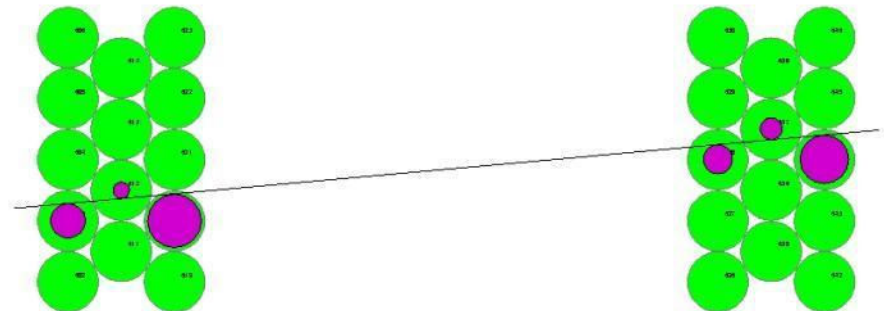
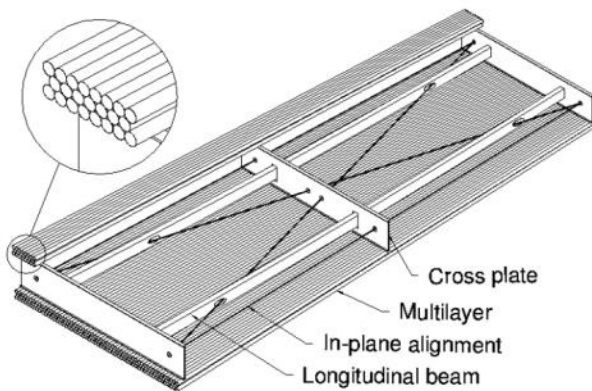


Electron avalanche at the wire.

The measured drift time is converted to a radius by a (calibrated) radius-time correlation.

Many of these circles define the particle track.

ATLAS Muon Chambers



ATLAS MDTs, $80\mu\text{m}$ per tube

The Geiger counter reloaded: Drift Tube

Atlas Muon Spectrometer, 44m long, from $r=5$ to 11m.

1200 Chambers

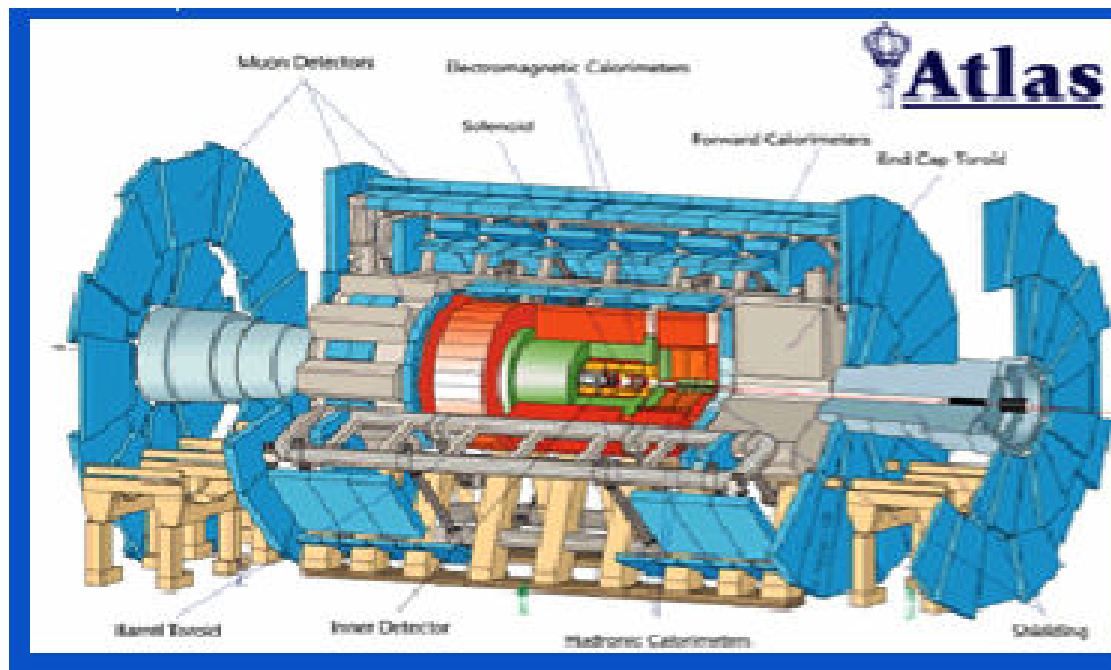
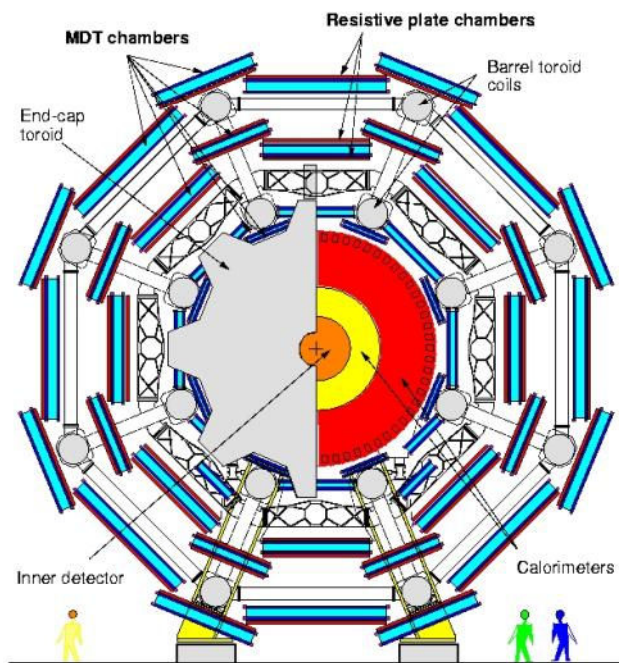
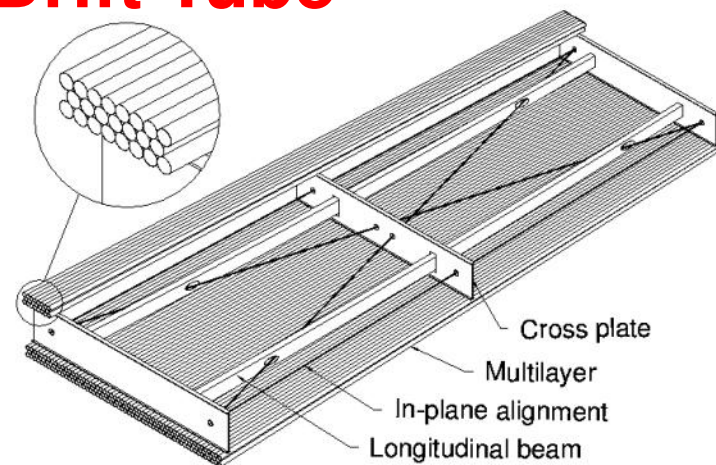
6 layers of 3cm tubes per chamber.

Length of the chambers 1-6m !

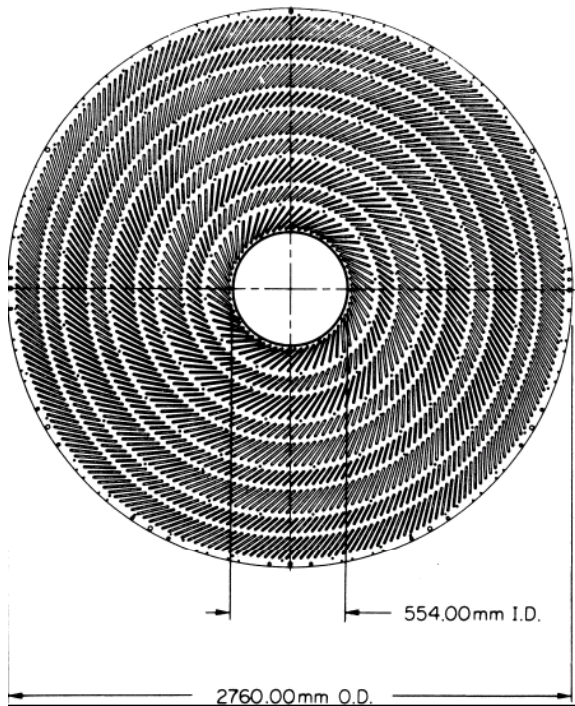
Position resolution: $80\mu\text{m}/\text{tube}$, $<50\mu\text{m}/\text{chamber}$ (3 bar)

Maximum drift time $\approx 700\text{ns}$

Gas Ar/CO₂ 93/7

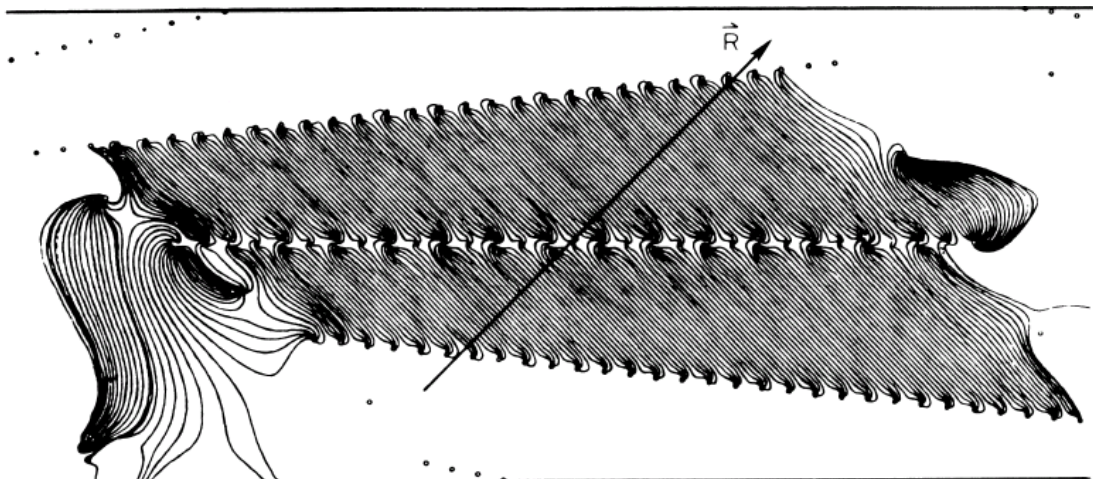


Large Drift Chambers



Central Tracking Chamber CDF
Experiment.

660 drift cells tilted 45° with respect to
the particle track.



Drift cell

Transport of Electrons in Gases: Drift-velocity

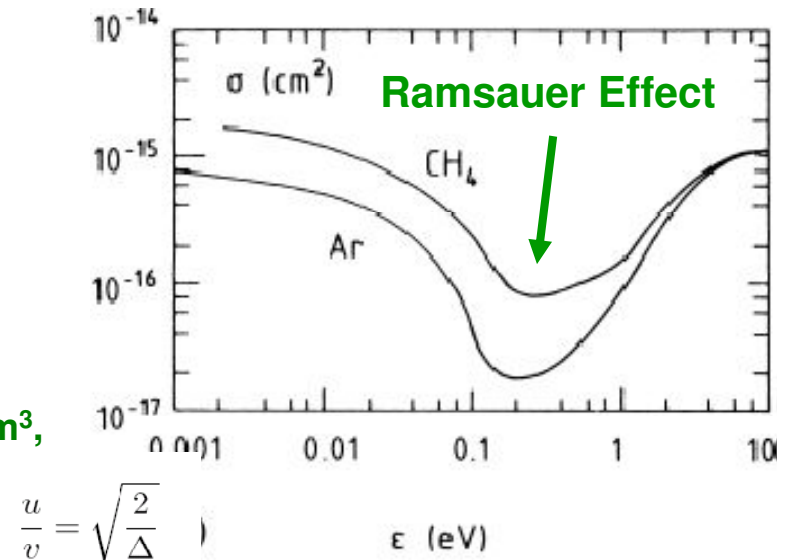
Electrons are completely 'randomized' in each collision. The actual drift velocity v along the electric field is quite different from the average velocity u of the electrons i.e. \rightarrow about 100 times smaller.

The velocities v and u are determined by the atomic crosssection $\sigma(\epsilon)$ and the fractional energy loss $\Delta(\epsilon)$ per collision (N is the gas density i.e. number of gas atoms/m³, m is the electron mass.):

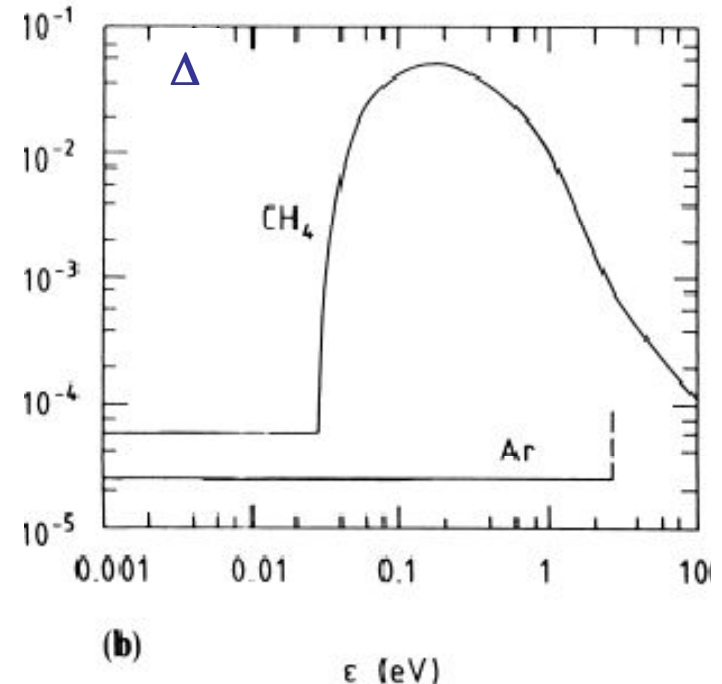
$$v = \sqrt{\frac{eE}{mN\sigma}} \sqrt{\frac{\Delta}{2}} \quad u = \sqrt{\frac{eE}{mN\sigma}} \sqrt{\frac{2}{\Delta}}$$

Because $\sigma(\epsilon)$ and $\Delta(\epsilon)$ show a strong dependence on the electron energy in the typical electric fields, the electron drift velocity v shows a strong and complex variation with the applied electric field.

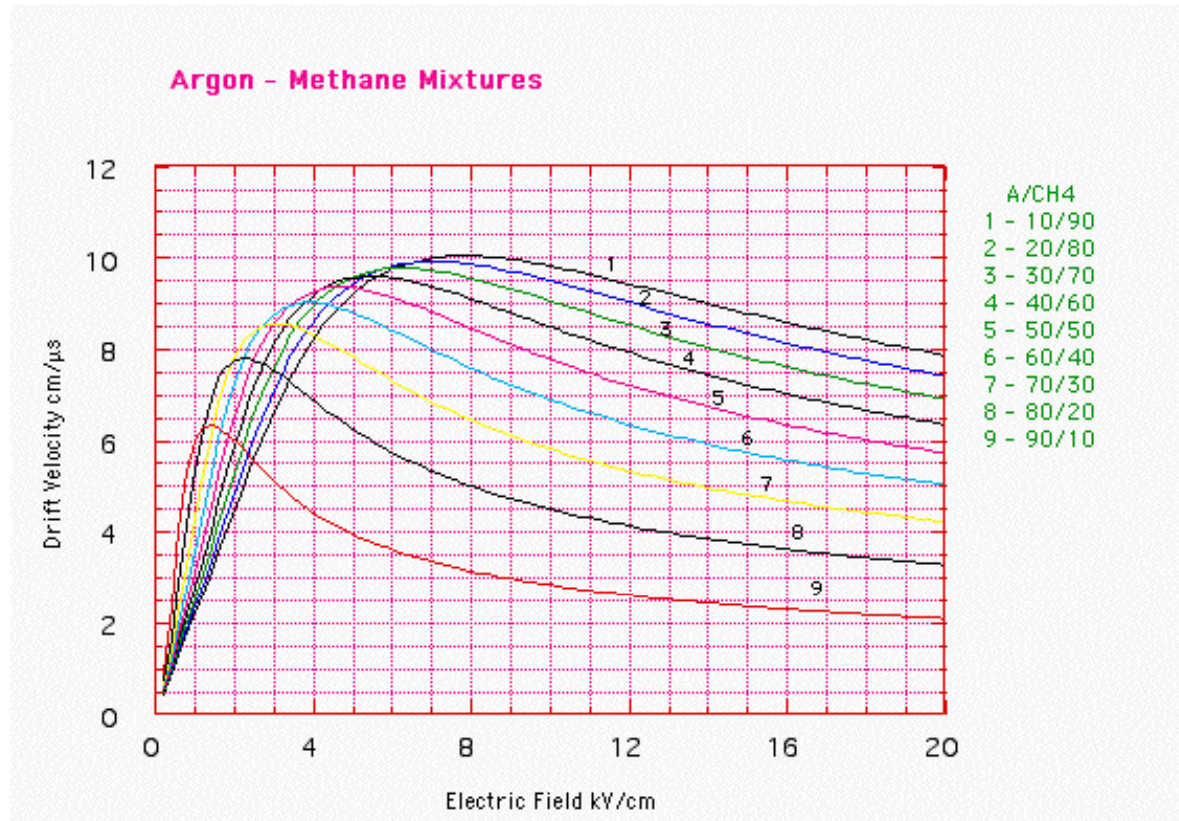
v is depending on E/N : doubling the electric field and doubling the gas pressure at the same time results in the same electric field.



$$\frac{u}{v} = \sqrt{\frac{2}{\Delta}}$$



Transport of Electrons in Gases: Drift-velocity

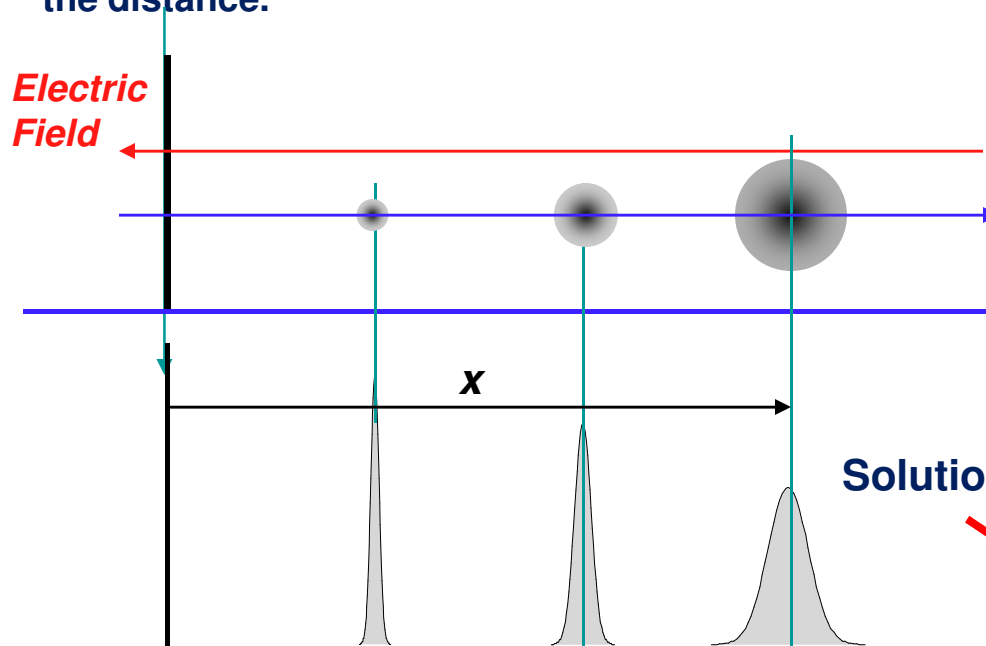


Typical Drift velocities are $v=5-10\text{cm}/\mu\text{s}$ (50 000-100 000m/s).
The microscopic velocity u is about ca. 100mal larger.

Only gases with very small electro negativity are useful (electron attachment)
→ Noble Gases (Ar/Ne) are most of the time the main component of the gas.
→ Admixture of CO_2 , CH_4 , Isobutane etc. for 'quenching' is necessary (avalanche multiplication – see later).

Transport of Electrons in Gases: Diffusion

An initially point like cloud of electrons will 'diffuse' because of multiple collisions and assume a Gaussian shape. The diffusion depends on the average energy of the electrons. The variance σ^2 of the distribution grows linearly with time. In case of an applied electric field it grows linearly with the distance.



$$n(x) = \left(\frac{1}{\sqrt{4\pi Dt}} \right)^3 e^{-\frac{(x-v_D t)^2}{4Dt}}$$

$$\sigma_x = \sqrt{2Dt}$$

Solution of the diffusion equation (l=drift distance)

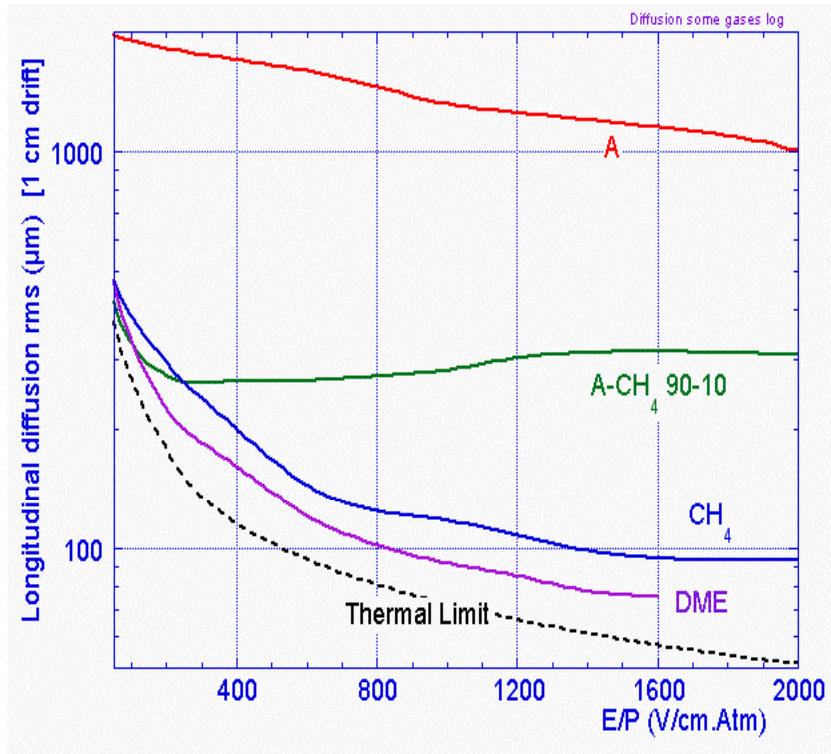
$$D = \frac{2}{3} \frac{v}{eE} \epsilon \quad \rightarrow \quad \sigma_x = \sqrt{\frac{4}{3} \frac{l}{eE} \epsilon}$$

Thermodynamic limit:

$$\epsilon = \frac{3}{2} kT \quad \rightarrow \quad \sigma_x = \sqrt{\frac{2kTl}{eE}}$$

Because $\epsilon = \epsilon(\mathbf{E}/P)$ $\sigma = \frac{1}{\sqrt{P}} F\left(\frac{E}{P}\right)$

Transport of Electrons in Gases: Diffusion



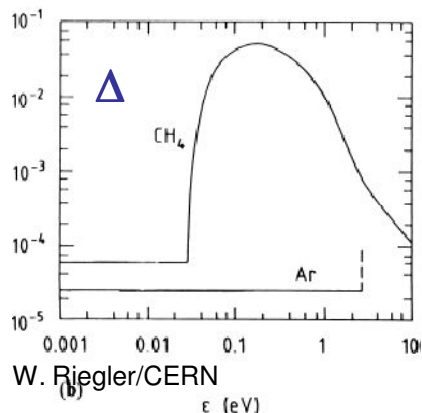
The electron diffusion depends on E/P and scales in addition with $1/\sqrt{P}$.

At 1kV/cm and 1 Atm Pressure the thermodynamic limit is $\sigma=70\mu\text{m}$ for 1cm Drift.

‘Cold’ gases are close to the thermodynamic limit i.e. gases where the average microscopic energy $\epsilon=1/2mu^2$ is close to the thermal energy $3/2kT$.

CH₄ has very large fractional energy loss \rightarrow low $\epsilon \rightarrow$ low diffusion.

Argon has small fractional energy loss/collision \rightarrow large $\epsilon \rightarrow$ large diffusion.



Drift of Ions in Gases

Because of the larger mass of the ions compared to electrons they are not randomized in each collision.

The cross sections are \approx constant in the energy range of interest.

Below the thermal energy the velocity is proportional to the electric field $v = \mu E$ (typical). Ion mobility $\mu \approx 1\text{-}10 \text{ cm}^2/\text{Vs}$.

Above the thermal energy the velocity increases with \sqrt{E} .

$V = \mu E$, $\mu(\text{Ar}) = 1.5 \text{ cm}^2/\text{Vs} \rightarrow 1000 \text{ V/cm} \rightarrow v = 1500 \text{ cm/s} = 15 \text{ m/s} \rightarrow 3000\text{-}6000$ times slower than electrons !

Time Projection Chamber (TPC):

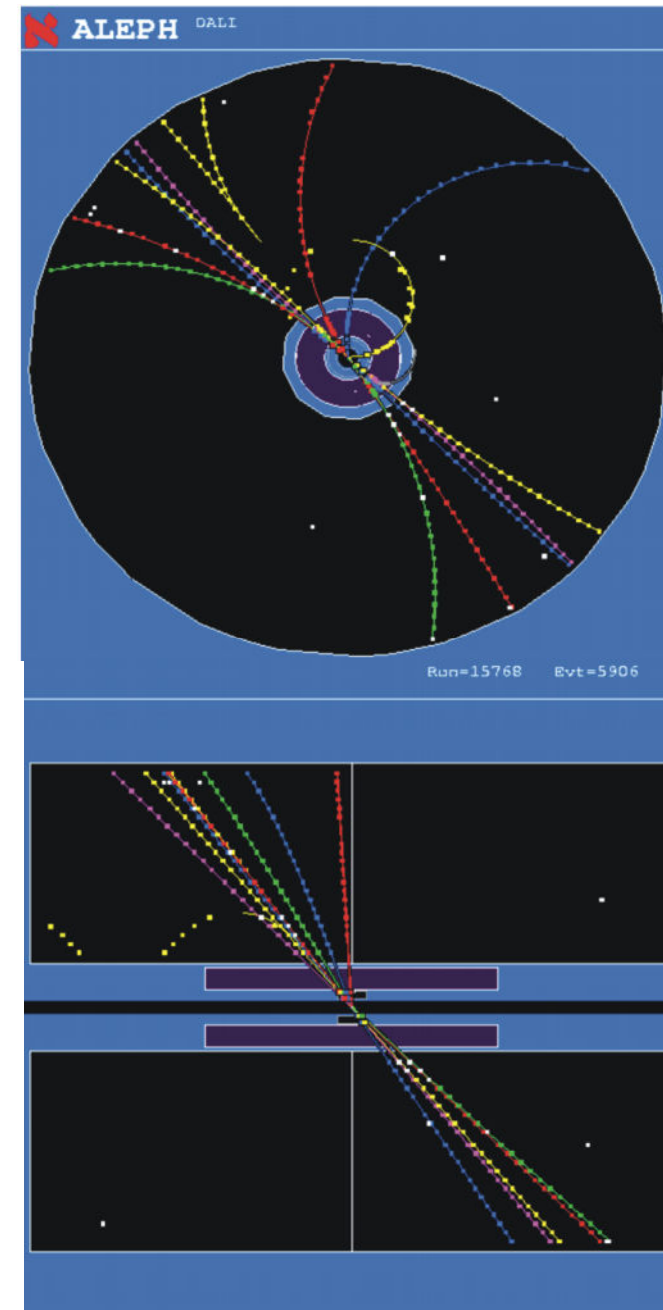
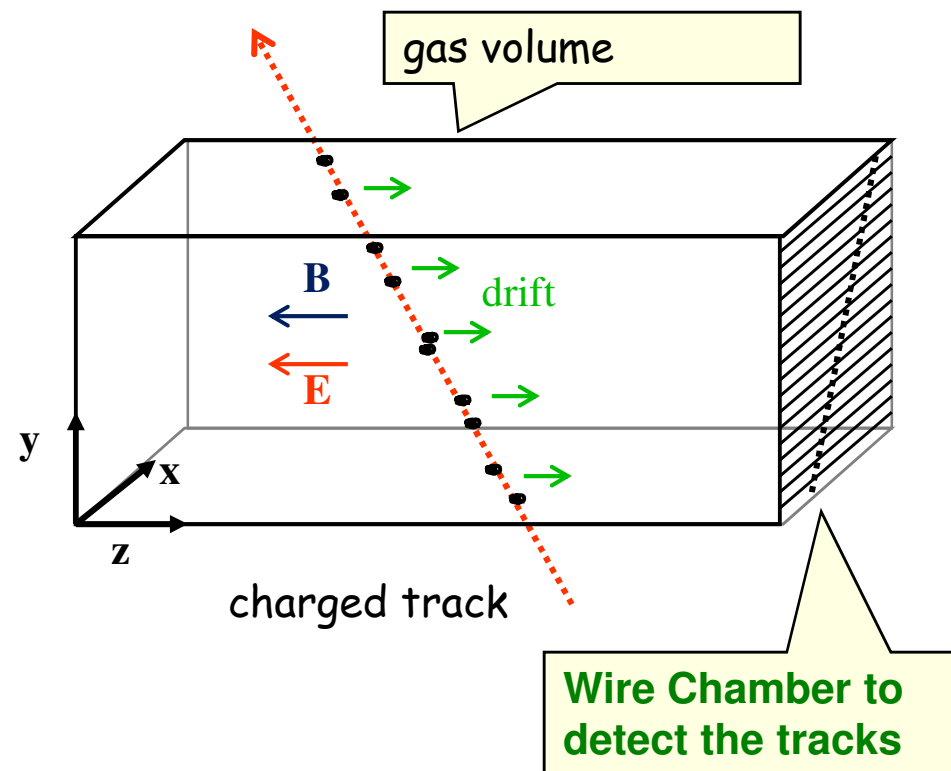
Gas volume with parallel E and B Field.

B for momentum measurement. Positive effect:

Diffusion is strongly reduced by E/B (up to a factor 5).

Drift Fields 100-400V/cm. Drift times 10-100 μs .

Distance up to 2.5m !

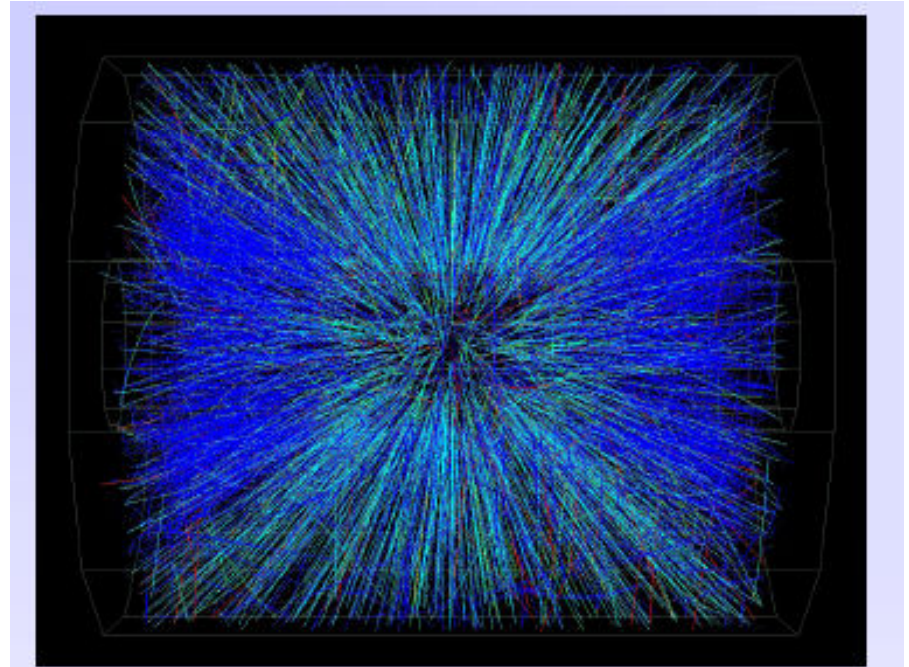
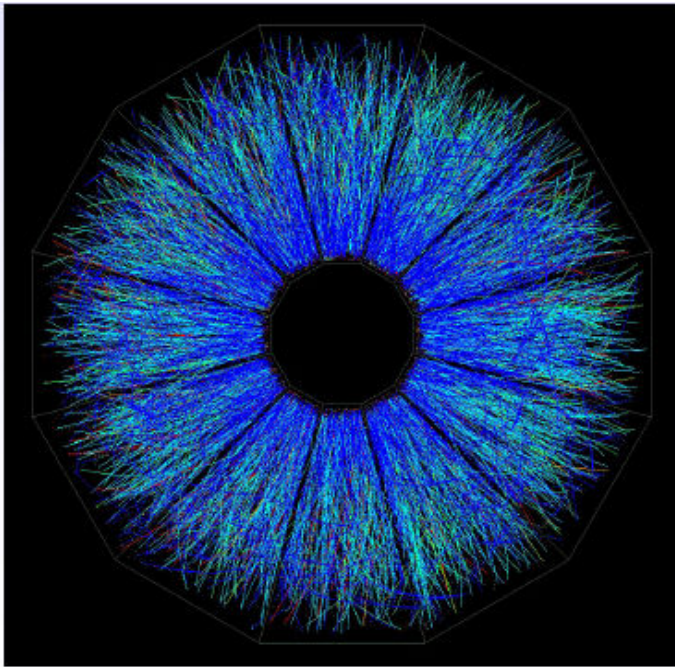


STAR TPC (BNL)

Event display of a Au Au collision at CM energy of 130 GeV/n.

Typically around 200 tracks per event.

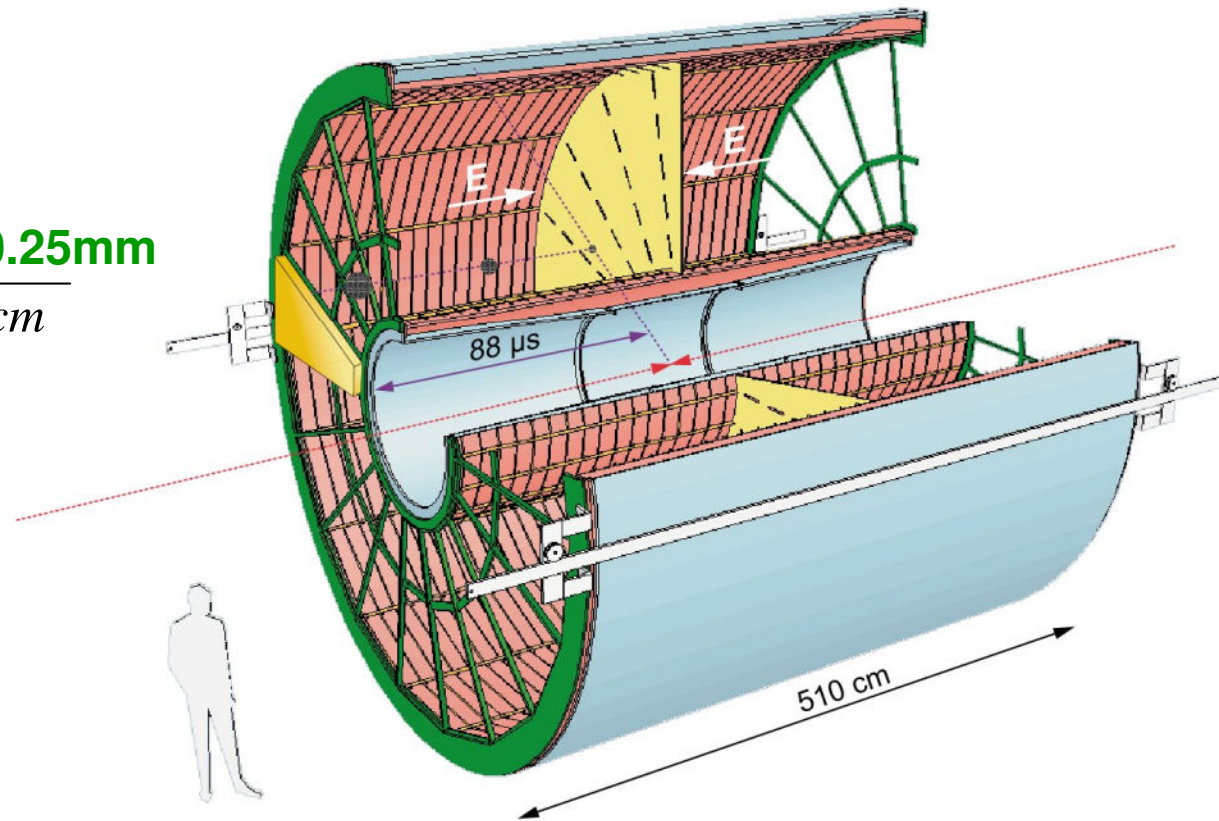
Great advantage of a TPC: The only material that is in the way of the particles is gas \rightarrow very low multiple scattering \rightarrow very good momentum resolution down to low momenta !



12/3/2009

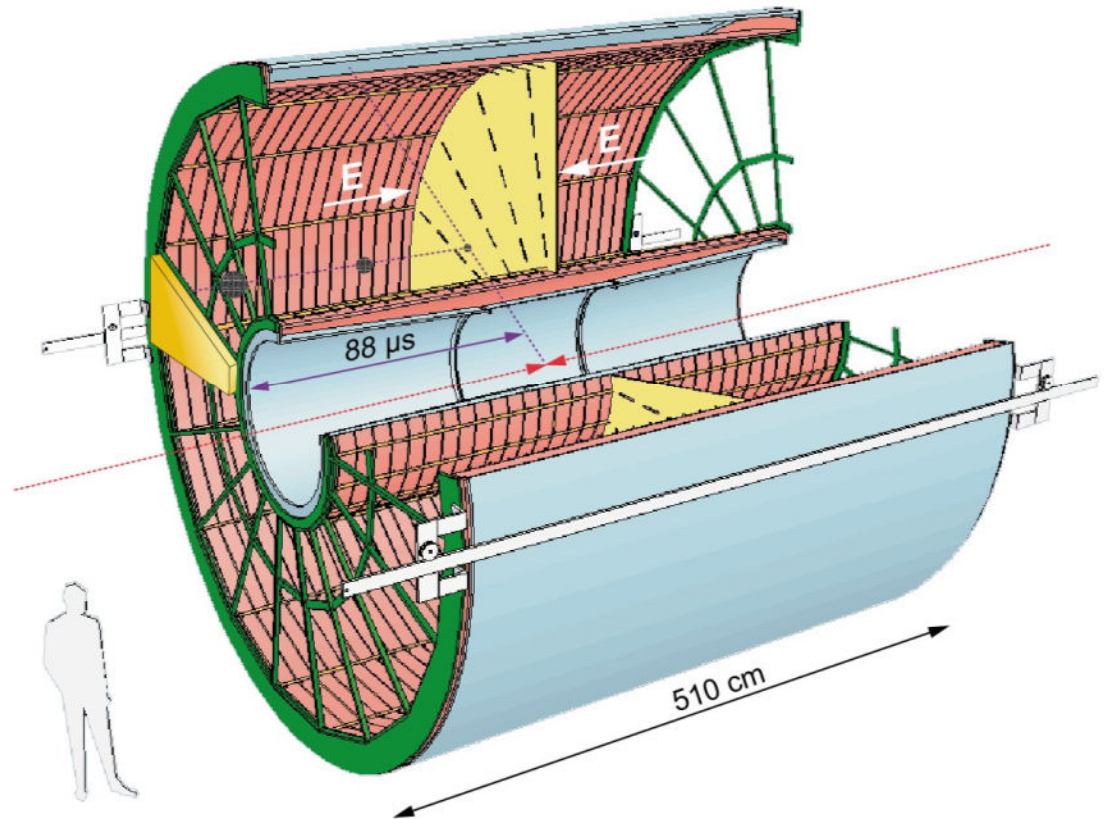
ALICE TPC: Detector Parameters

- Gas Ne/ CO₂ 90/10%
- Field 400V/cm
- Gas gain $>10^4$
- Position resolution $\sigma = 0.25\text{mm}$
- Diffusion: $\sigma_t = 250\mu\text{m} \sqrt{cm}$
- Pads inside: 4x7.5mm
- Pads outside: 6x15mm
- B-field: 0.5T



ALICE TPC: Construction Parameters

- **Largest TPC:**
 - Length 5m
 - Diameter 5m
 - Volume 88m³
 - Detector area 32m²
 - Channels ~570 000
- **High Voltage:**
 - Cathode -100kV
- **Material X_0**
 - Cylinder from composite materials from airplane industry ($X_0 = \sim 3\%$)



ALICE TPC: Pictures of the Construction

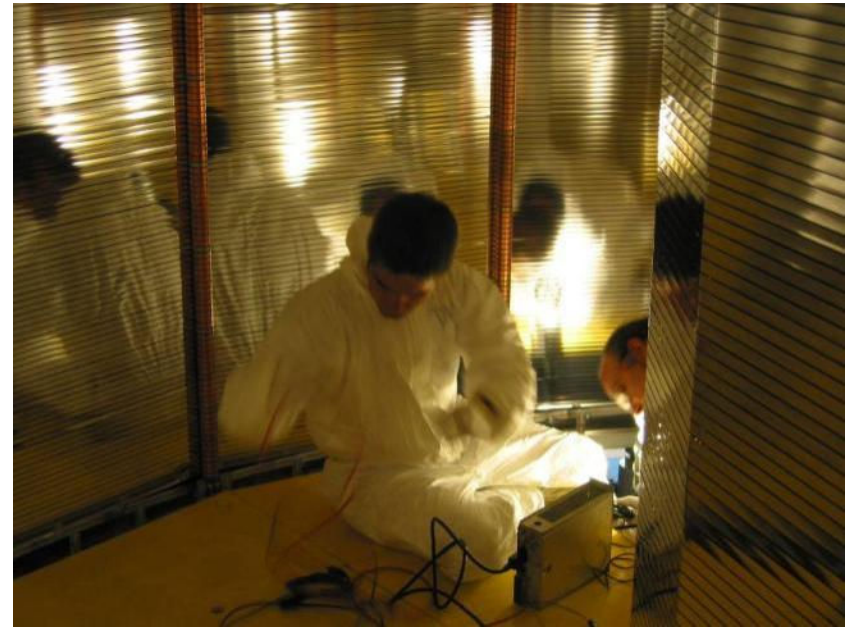
Precision in z: $250\mu\text{m}$



End plates $250\mu\text{m}$



Wire chamber: $40\mu\text{m}$



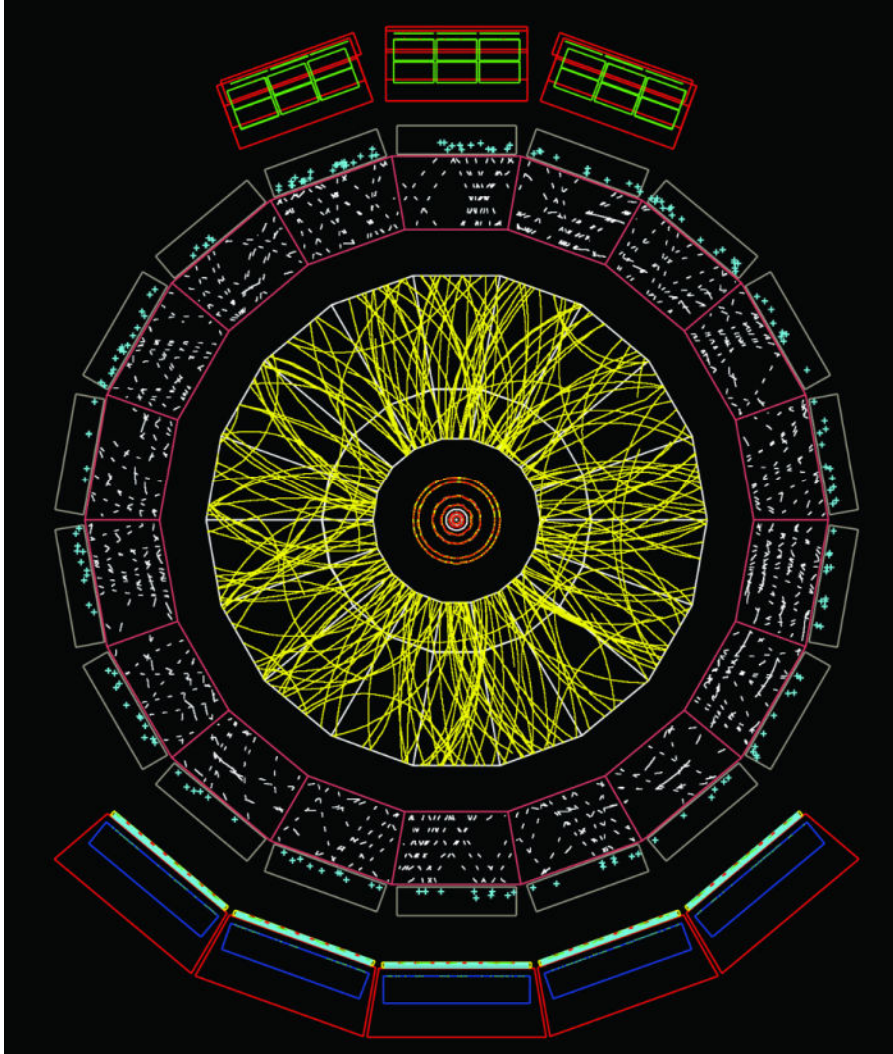
ALICE TPC Construction

My personal
contribution:

A visit inside the TPC.

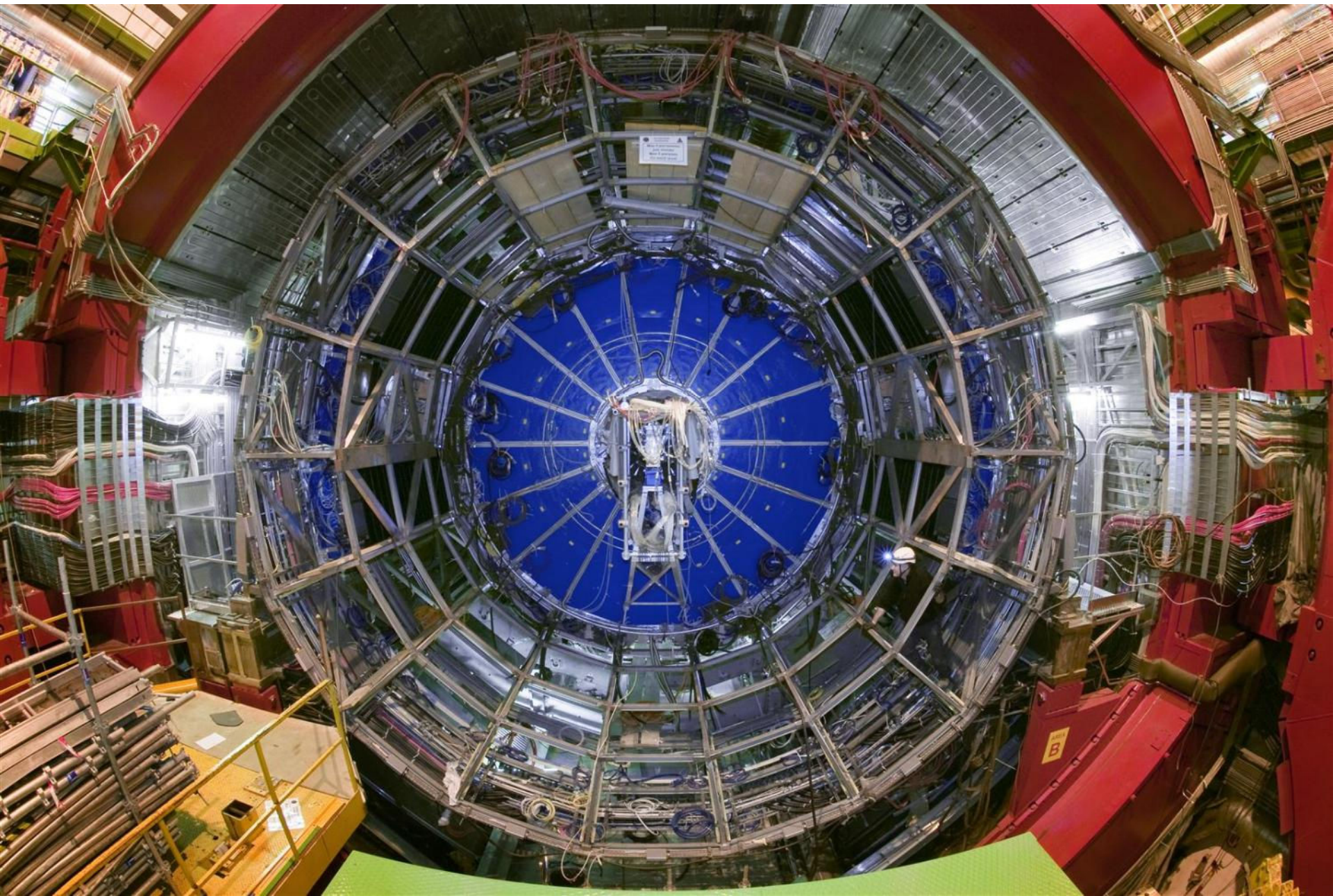


ALICE : Simulation of Particle Tracks

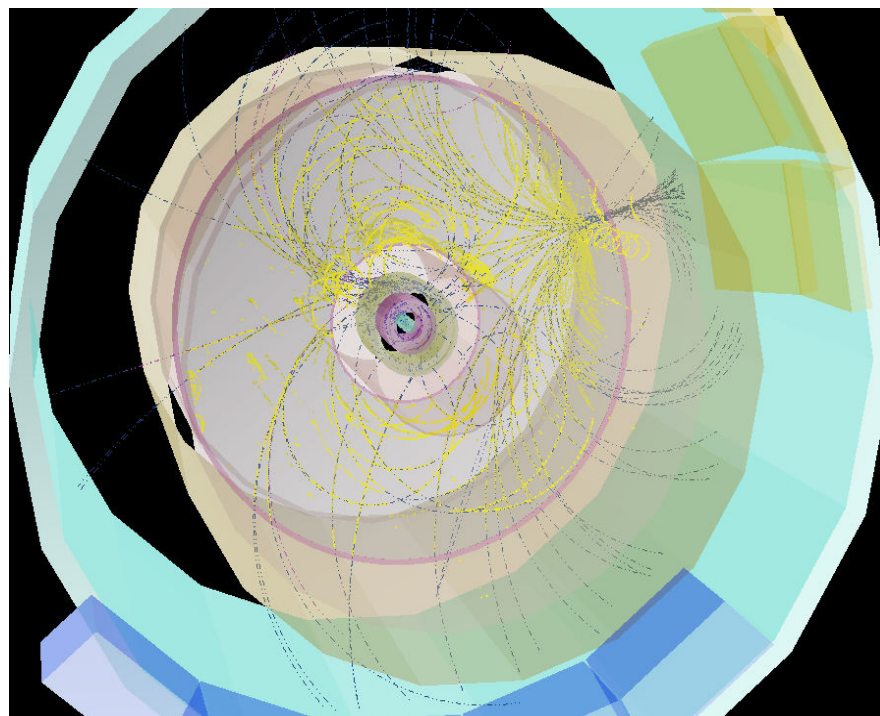
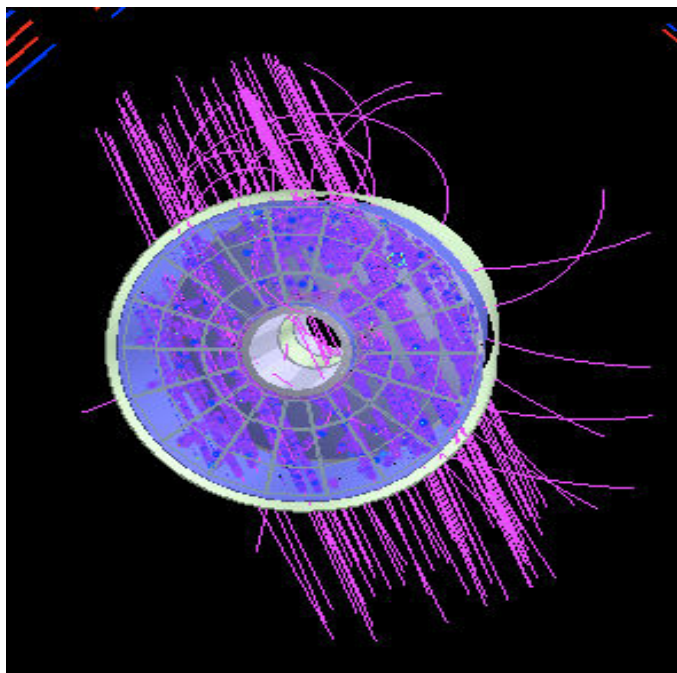
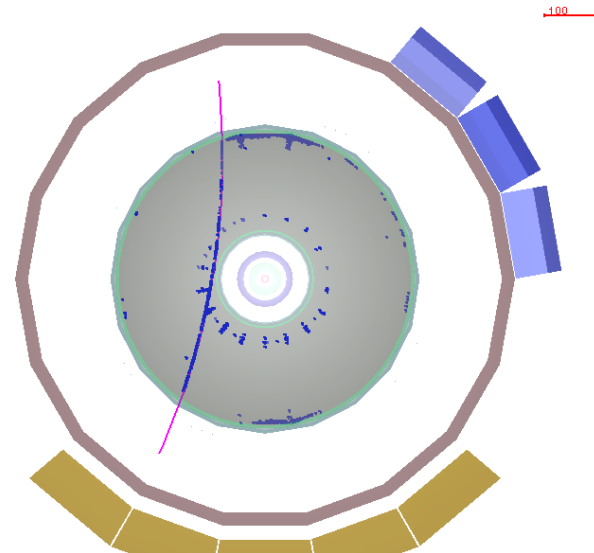
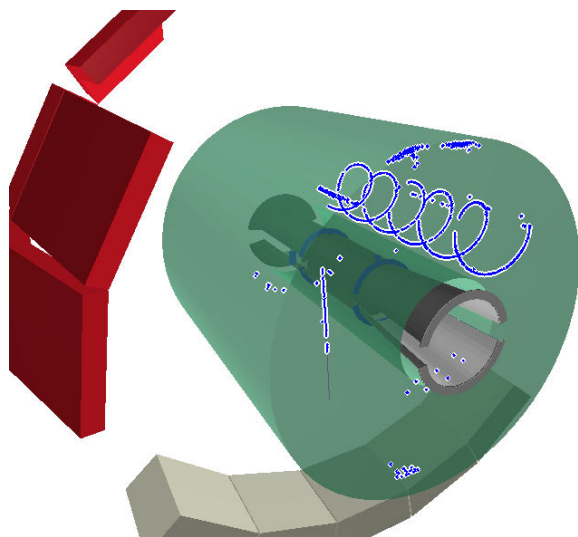


- Simulation of particle tracks for a Pb Pb collision ($dN/dy \sim 8000$)
- Angle: $\Theta = 60$ to 62°
- If all tracks would be shown the picture would be entirely yellow !
- Up to 40 000 tracks per event !
- TPC is currently under commissioning

TPC installed in the ALICE Experiment



First Cosmic Muon Event Displays from the ALICE TPC June 2008 !



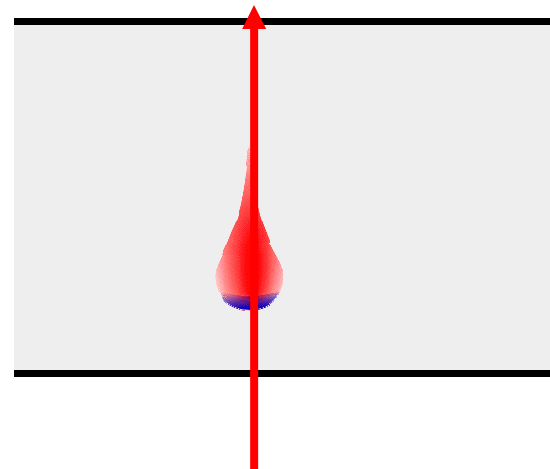
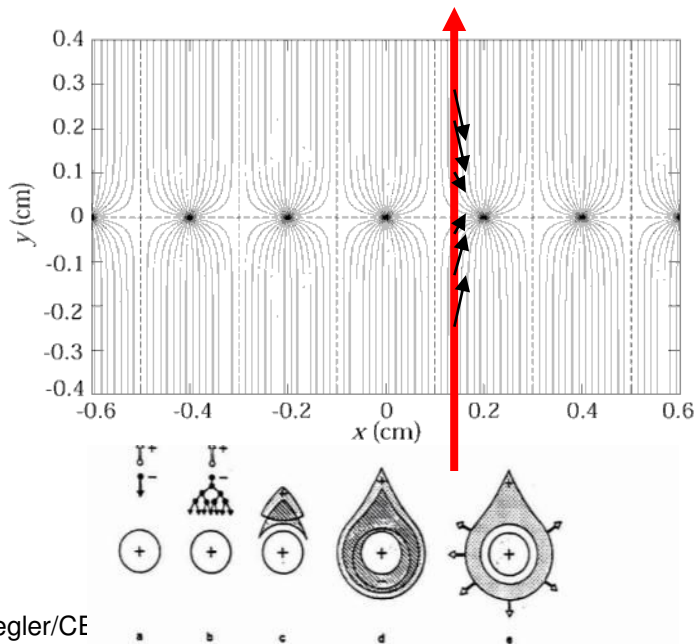
Position Resolution/Time resolution

Up to now we discussed gas detectors for tracking applications. Wire chambers can reach tracking precisions down to 50 micrometers at rates up to $<1\text{MHz/cm}^2$.

What about time resolution of wire chambers ?

It takes the electrons some time to move from their point of creation to the wire. The fluctuation in this primary charge deposit together with diffusion limits the time resolution of wire chambers to about 5ns (3ns for the LHCb trigger chambers).

By using a parallel plate geometry with high field, where the avalanche is starting immediately after the charge deposit, the timing fluctuation of the arriving electrons can be eliminated and time resolutions down to 50ps can be achieved !



Resistive Plate Chambers (RPCs)

Keuffel 'Spark' Counter:

High voltage between two metal plates. Charged particle leaves a trail of electrons and ions in the gap and causes a discharge (Spark).

→ Excellent Time Resolution (<100ps).

Discharged electrodes must be recharged → Dead time of several ms.

Parallel Plate Avalanche Chambers (PPAC):

At more moderate electric fields the primary charges produce avalanches without forming a conducting channel between the electrodes. No Spark → induced signal on the electrodes. Higher rate capability.

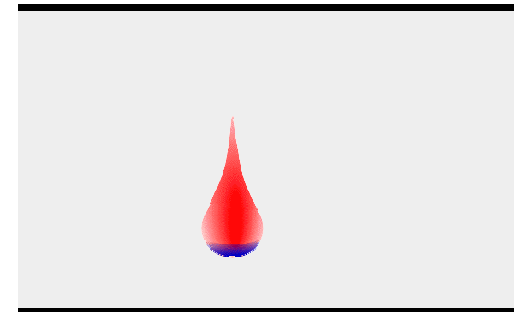
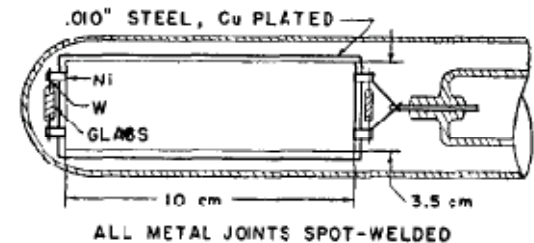
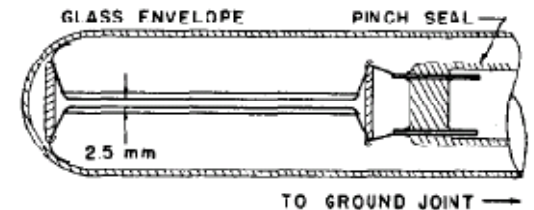
However, the smallest imperfections on the metal surface cause sparks and breakdown.

→ Very small (few cm²) and unstable devices.

In a wire chamber, the high electric field (100-300kV/cm) that produces the avalanche exists only close to the wire. The fields on the cathode planes are rather small 1-5kV/cm.

Parallel-Plate Counters

J. WARREN KEUFFEL*
California Institute of Technology, Pasadena, California
(Received November 8, 1948)



Resistive Plate Chambers (RPCs)

→ Place resistive plates in front of the metal electrodes.

No spark can develop because the resistivity together with the capacitance ($\tau \sim \epsilon \cdot \rho$) will only allow a very localized 'discharge'. The rest of the entire surface stays completely unaffected.

→ Large area detectors are possible !

Resistive plates from Bakelite ($\rho = 10^{10}$ - $10^{12} \Omega\text{cm}$) or window glass ($\rho = 10^{12}$ - $10^{13} \Omega\text{cm}$).

Gas gap: 0.25-2mm.

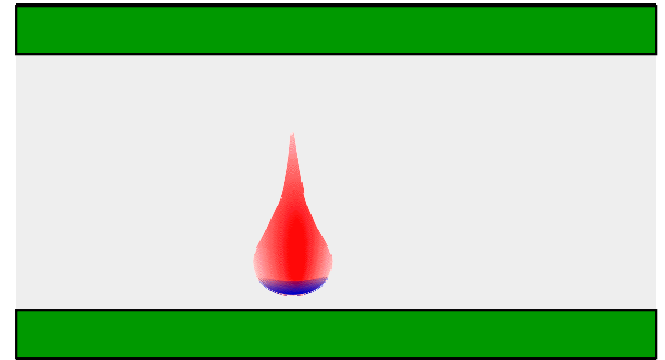
Electric Fields 50-100kV/cm.

Time resolutions: 50ps (100kV/cm), 1ns(50kV/cm)

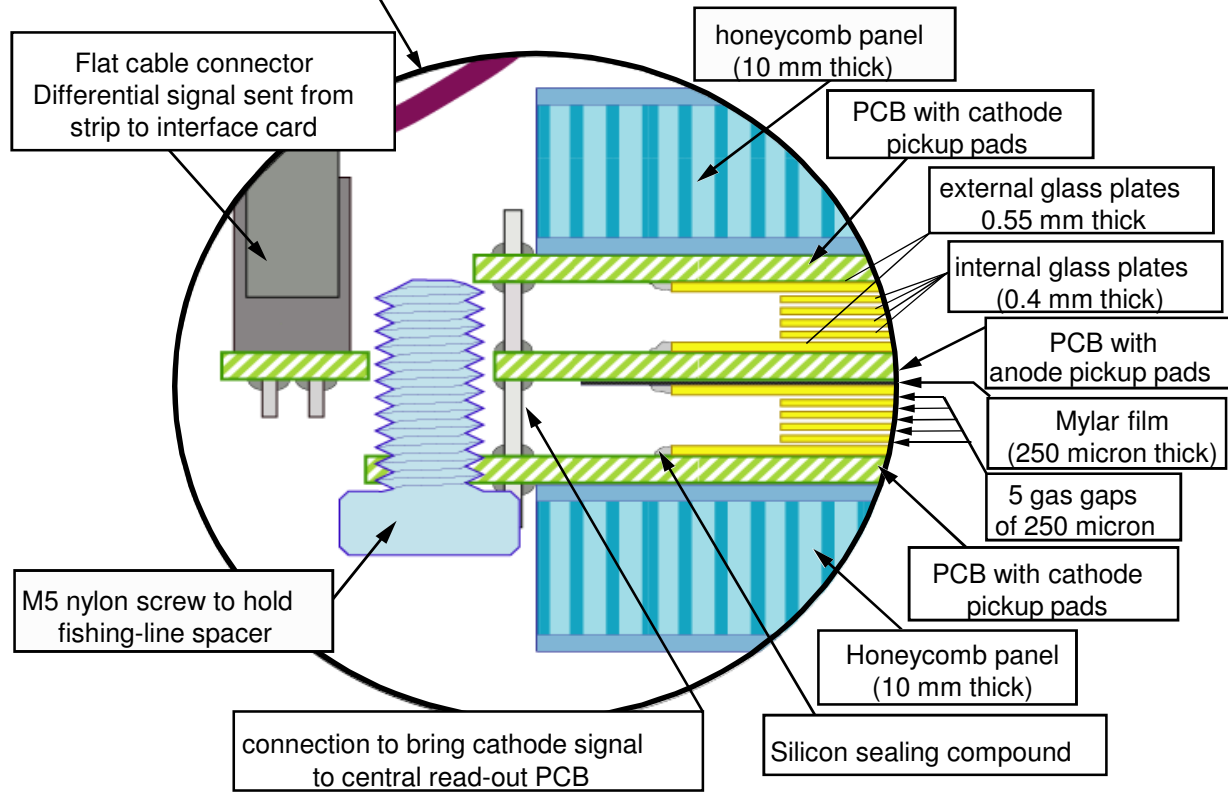
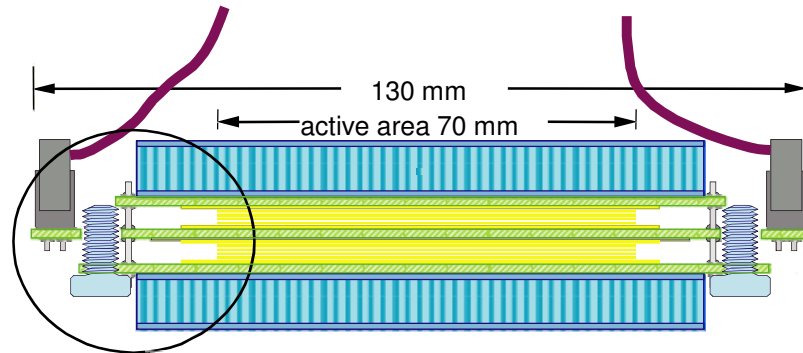
Application: Trigger Detectors, Time of Flight (TOF)

Resistivity limits the rate capability: Time to remove avalanche charge from the surface of the resistive plate is ($\tau \sim \epsilon \cdot \rho$) = ms to s.

Rate limit of kHz/cm² for $10^{10} \Omega\text{cm}$.



ALICE TOF RPCs



Several gaps to increase efficiency.
Stack of glass plates.

Small gap for good time resolution:
0.25mm.

Fishing lines as high precision
spacers !

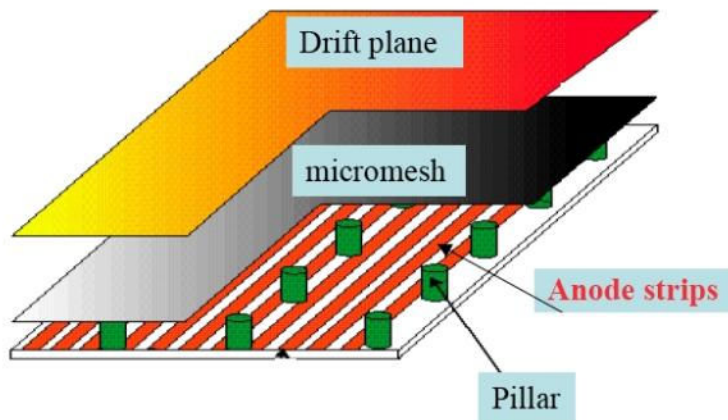
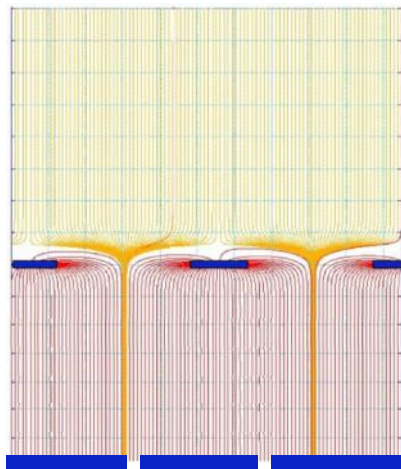
Large TOF systems with 50ps time
resolution made from window glass
and fishing lines !

Before RPCs → Scintillators with very
special photomultipliers – very
expensive. Very large systems are
unaffordable.

GEMs & MICROMEGAS

MICROMEGAS

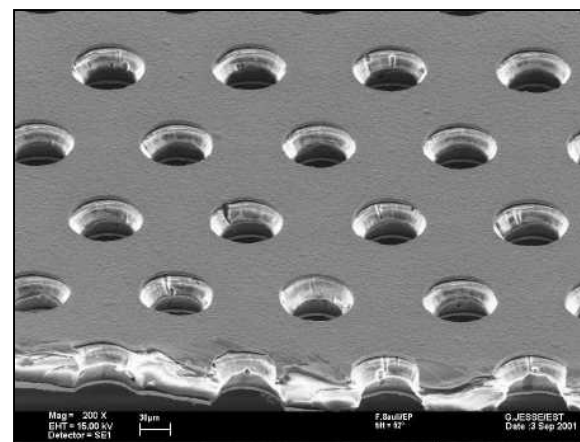
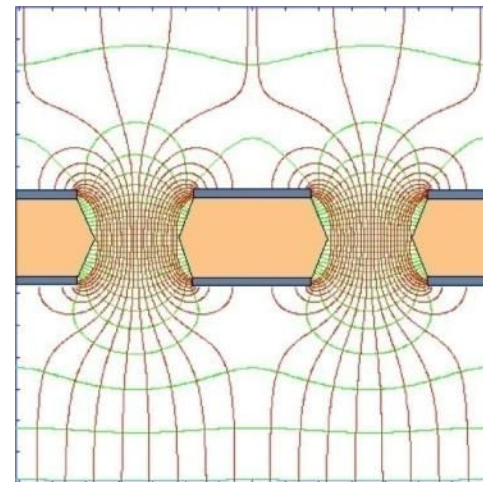
Narrow gap (50-100 μm) PPC with thin cathode mesh
Insulating gap-restoring wires or pillars



Y. Giomataris et al, Nucl. Instr. and Meth. A376(1996)239
12/3/2009

GEM

Thin metal-coated polymer foils
70 μm holes at 140 mm pitch

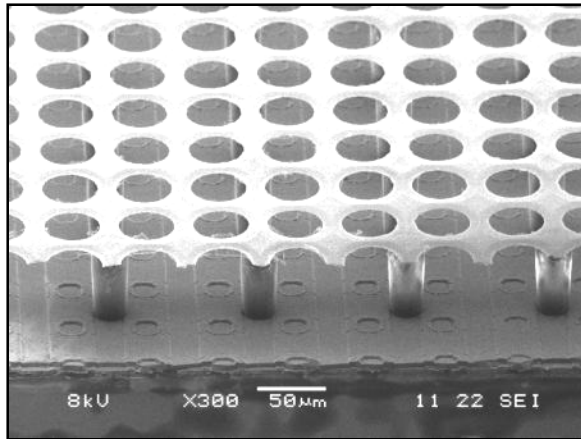


F. Sauli, Nucl. Instr. and Methods A386(1997)531

MPGDs with Integrate Micromesh, INGRID

Going even another step further, by wafer post-processing techniques, MPGD structure can be put on top of a pixelized readout chip, making the entire detector a monolithic unit !

→ IntegratedGrid (INGRID) . In addition a TDC was put on each pixel measuring drift times →

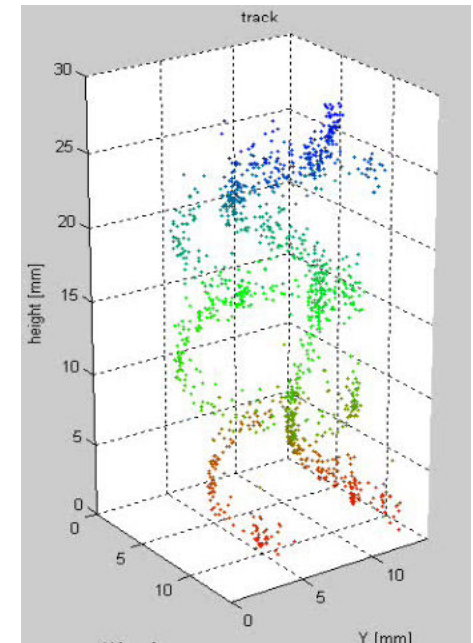
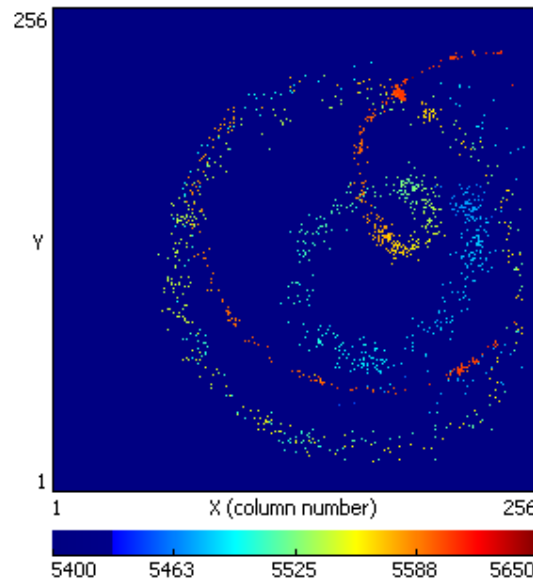


Micromesh on a pixelized readout chip produced by Opto-Chemical Wafer Post-Processing Techniques.

With 3cm Drift gap: 5 cm³ Mini TPC !
Tracks from Sr90 source in 0.2T
Magnetic Field !

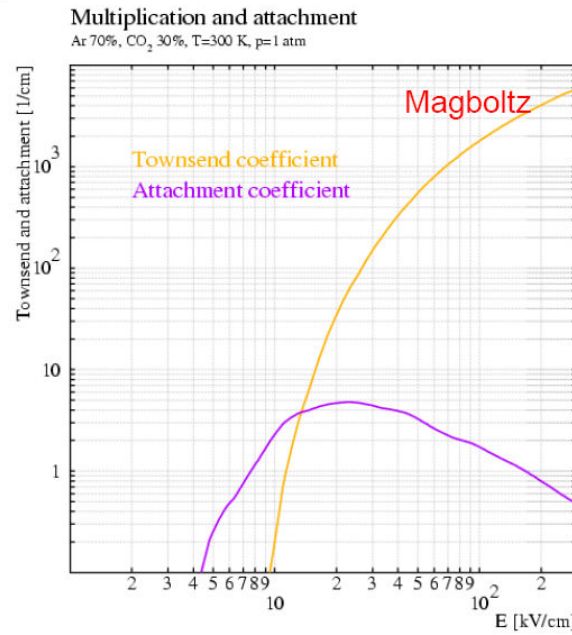
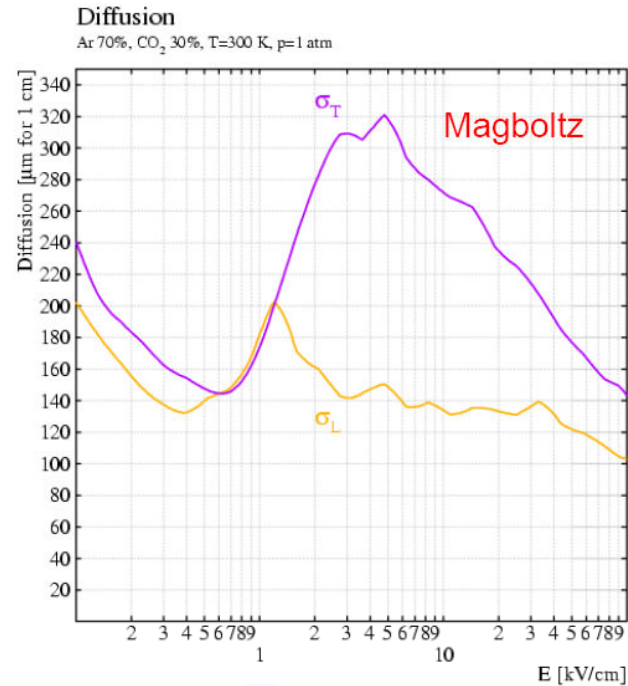
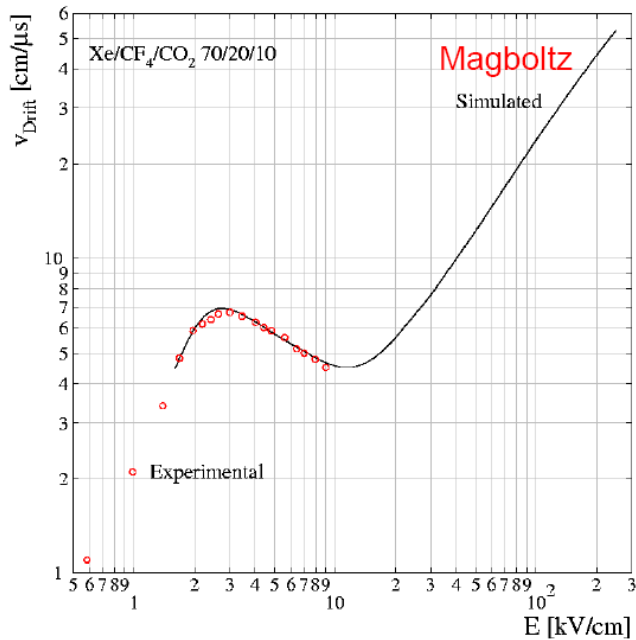
Single ionization electrons are seen.

Fantastic position resolution ...



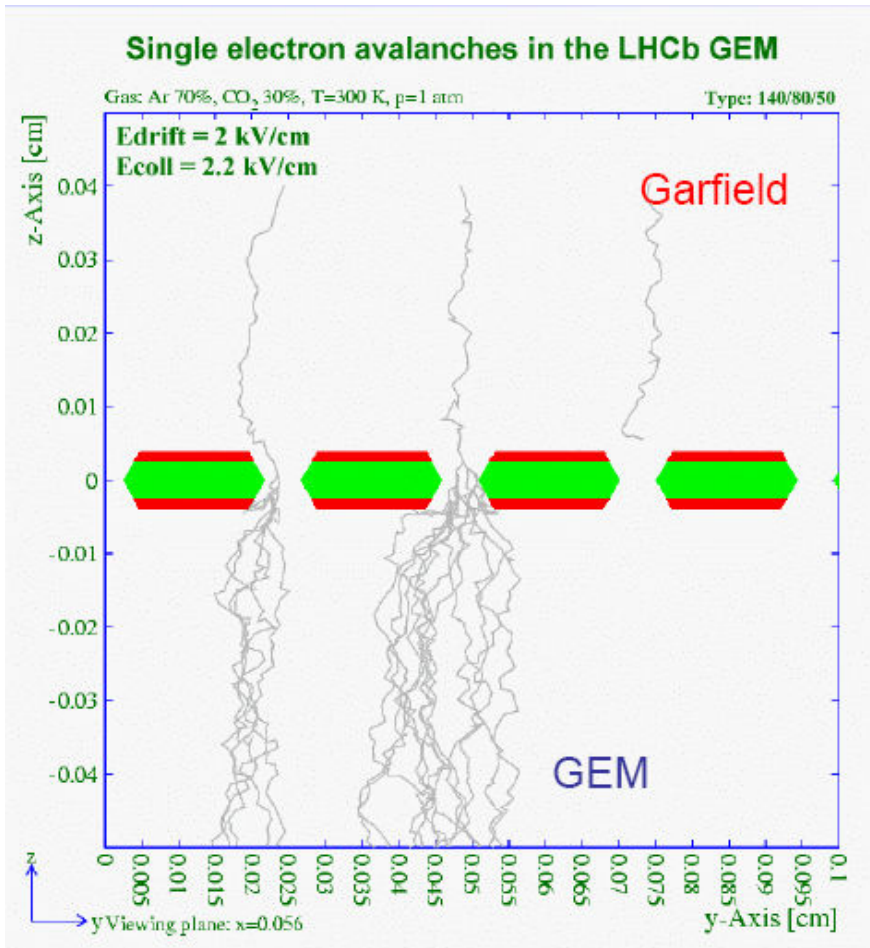
12/3/2009

Detector Simulation

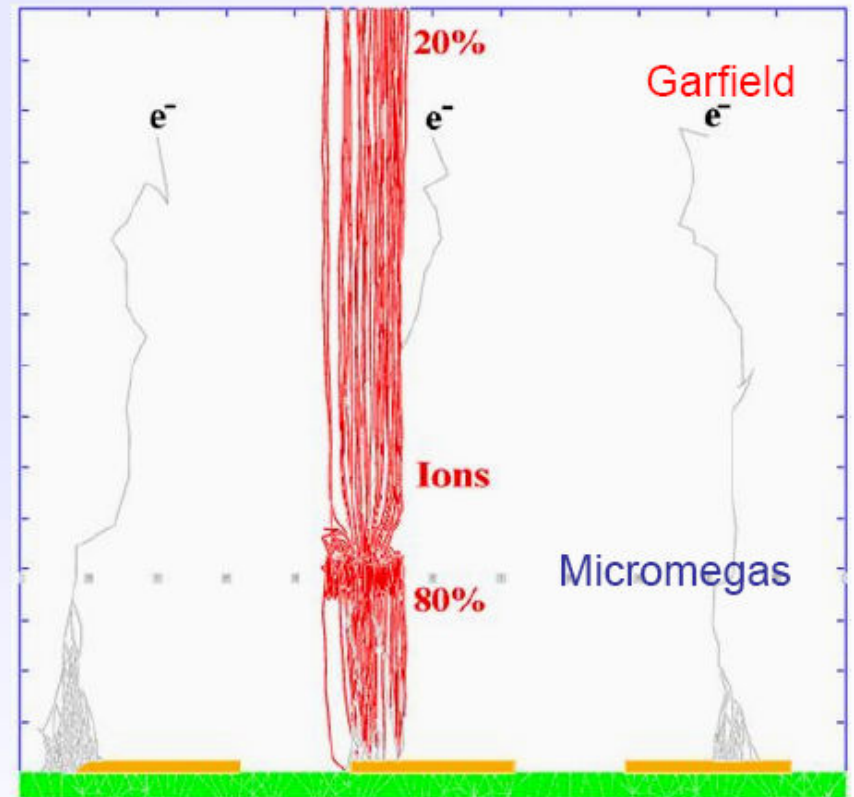


12/3/2009

Detector Simulation



Electrons paths and multiplication



Positive ion backflow

12/3/2009

Summary on Gas Detectors

Wire chambers feature prominently at LHC. A decade of very extensive studies on gases and construction materials has lead to wire chambers that can track up to MHz/cm^2 of particles, accumulate up to $1\text{-}2\text{C/cm}$ of wire and $1\text{-}2\text{ C/cm}^2$ of cathode area.

While silicon trackers currently outperform wire chambers close to the interaction regions, wire chambers are perfectly suited for the large detector areas at outer radii.

Large scale next generation experiments foresee wire chambers as large area tracking devices.

The Time Projection Chamber – if the rate allows it's use – is unbeatable in terms of low material budget and channel economy. There is no reason for replacing a TPC with a silicon tracker.

Gas detectors can be simulated very accurately due to excellent simulation programs.

Novel gas detectors, the Micro Pattern Gas Detectors, have proven to work efficiently as high rate, low material budget trackers in the 'regime' between silicon trackers and large wire chambers.

12/3/2009